~~New~~ Eevidence for millennial-scale interactions between Hg cycling and hydroclimate from Lake Bosumtwi, Ghana

Alice R. Paine[1,2]*, Joost Frieling[1], Timothy M. Shanahan[2], Tamsin A. Mather[1], Nicholas McKay[3], Stuart A. Robinson[1], David M. Pyle[1], Isabel M. Fendley[1], Ruth Kiely[4], William D. Gosling[4]

[1]Department of Earth Sciences, University of Oxford, UK, OX1 3AN
[2]*Department of Environmental Sciences, University of Basel, Bernoullistrasse 32, CH-4056 Basel, Switzerland
[3][2]Department of Earth and Planetary Sciences, University of Texas at Austin, Texas, USA
[4][3]School of Earth and Sustainability, Northern Arizona University, Flagstaff, Arizona, USA
[5][4]Institute for Biodiversity & Ecosystem Dynamics, University of Amsterdam, Amsterdam, Netherlands

Corresponding Author: alice.paine@unibas.ch
current affiliation~~*Corresponding Author: alice.paine@earth.ox.ac.uk~~

Changing hydrology impacts the biogeochemical cycling of elements such as mercury (Hg), whose transport and transformation in the environment appear linked to hydroclimate on diverse timescales. Key questions remain about how these processes manifest over different timescales and their potential environmental consequences. For example, millennial-scale Hg-hydroclimate interactions in the terrestrial realm are poorly understood, as few sedimentary records have sufficient length and/or resolution to record abrupt and long-lasting changes in Hg cycling, and the relative roles of depositional processes on these changes. Here, we present a high-resolution sedimentary Hg record from tropical Lake Bosumtwi (Ghana, West Africa) since ~96 ka. A coupled response is observed between Hg flux and shifts in sediment composition, the latter reflecting changes in lake level. Specifically, we find that the amplitude and frequency of Hg peaks increase as the lake level rises, suggesting that Hg burial was enhanced in response to an insolation-driven increase in precipitation at ~73 ka. A more transient, threefold increase in Hg concentration and accumulation rate is also recorded between ~13 and 4 ka, coinciding with a period of distinctly higher rainfall across North Africa known as the African Humid Period. Two mechanisms, likely working in tandem, could explain this correspondence: (1) an increase in wet deposition of Hg by precipitation and (2) efficient sequestration of organic-hosted Hg. Taken together, our results reaffirm that changes in hydroclimate, directly and/or indirectly, can be linked to millennial-scale changes in tropical Hg cycling, and that these signals can be recorded in lake sediments.

KEYWORDS: lacustrine, geochemistry, sediment, sapropel, organic, Africa

1. Introduction

38   Mercury (Hg) is a volatile and toxic metal released into the atmosphere as a result of natural
39   processes (e.g., volcanism, geothermal activity, weathering; Edwards et al., 2021; Selin, 2009) and,
40   more recently, human activities (e.g., industrial activities, mining, coal burning; Amos et al., 2015).
41   Approximately 95 % of atmospheric Hg exists in gaseous elemental form (Hg^0). An atmospheric
42   lifetime of up to 2 years permits its transport over long distances prior to removal by wet or dry
43   deposition, and following oxidation and aerosol scavenging (Lyman et al., 2020). Once free gaseous
44   (Hg^0) and/or oxidised (Hg^{II}) Hg has been deposited into the terrestrial environment, two sets of
45   reactions become particularly important: (1) oxidation-reduction, and (2) methylation-demethylation
46   (Branfireun et al., 2020). The reduction of Hg^{II} to Hg^0 can result in release back into the atmosphere.
47   Hg^{II} can also be bound to organic matter (OM) or sulphides, and thus be sequestered and
48   accumulated in sediments (Åkerblom et al., 2013; Hsu-Kim et al., 2013; Mason et al., 2000).
49   Accumulation of Hg in the terrestrial environment is therefore a function of the balance between Hg
50   removal from and re-emission to the atmosphere, and governed by the rate and intensity of different
51   thermal, photo, and biogenic reactions (Bishop et al., 2020; Obrist et al., 2018).

52   The exchange of Hg between the terrestrial biosphere, hydrosphere, critical zone, and atmosphere
53   are intrinsically coupled to climate. Changes in ecosystem Hg loading, overland transport, and
54   methylation have all been directly linked to decadal-scale changes in global temperature and
55   precipitation, and their associated shifts in terrestrial productivity, land-atmosphere exchange, and
56   wildfire dynamics (Bishop et al., 2020; Li et al., 2020). However, studying the long-term natural Hg
57   cycle presents several challenges. For example, the overwhelming increase in anthropogenic Hg
58   fluxes in recent decades have substantially altered the environmental dynamics of this cycle,
59   complicating assessment of how long-term climate change may alter its rate, intensity, and evolution
60   (United Nations Environment Programme, 2018). Pre-industrial-age archives allow for clear
61   comparison between natural and anthropogenic-driven changes in Hg cycling, and identification of
62   which regions may be most vulnerable to the negative effects of these changes, and highlight the
63   importance of understanding the long-term Hg cycle (e.g., Cooke et al., 2020; Segato et al., 2023).

64

1.1 Mercury cycling and hydroclimate.

66   The transport and transformation of Hg at the Earth's surface is ~~directly~~ linked to the hydrological
67   cycle (Bishop et al., 2020; Selin, 2009). Water plays a direct role in the efficiency of both Hg
68   deposition and re-emission. For example, changes in precipitation ~~patterns~~ amount can influence the
69   proportion of Hg removed from the atmosphere by wet versus dry deposition, with higher precipitation
70   amounts generally corresponding to enhanced Hg deposition at the surface (Amos et al., 2015;
71   Guédron et al., 2018). Elevated Hg concentrations have been measured in equatorial ocean surface
72   waters corresponding to inter-annual peaks in precipitation, with general circulation model simulations
73   suggesting that these are likely due to higher net Hg flux by wet deposition (Kuss et al., 2011;
74   Soerensen et al., 2014; Sprovieri et al., 2010). Multi-year monitoring by the Global Mercury
75   Observation System (GMOS) has similarly revealed distinct interannual differences in total wet

76 deposition of Hg, with the highest fluxes typically occurring in the wettest years (Leiva González et al.,
77 2022; Sprovieri et al., 2017). Precipitation also facilitates Hg transport in terrestrial watersheds, with
78 simultaneous increases in river discharge, surface runoff, and soil erosion during and after intense
79 storm events all enhancing hydrological 'connectivity' between surface environments and feeder
80 tributaries (Bishop et al., 2020). This enhances overland transport of Hg and other suspended
81 materials, and subsequently their delivery to lake and near-shore marine sediments (Liu et al., 2021;
82 Zaferani and Biester, 2021).

83 Water also plays an indirect role in drawdown and sequestration of Hg in aquatic environments.
84 Systems that are particularly sensitive to changes in water balance (e.g., terrestrial lakes) are most
85 likely to experience distinct, hydro-climate driven environmental changes that impact their internal Hg
86 cycle (Branfireun et al., 2020). For example, changes in organic matter cycling between the
87 catchment and the lake (Ravichandran, 2004), algal scavenging (Outridge et al., 2019), and early
88 diagenesis (Frieling et al., 2023). A decline in the total water volume of a basin may also elicit a
89 reduction in stratification (Woolway et al., 2020), during which increased mixing would ventilate
90 bottom waters and reduce organic-matter burial (Gulati et al., 2017). Conversely, a simultaneous
91 increase in total water volume and nutrient influx may increase stratification and bottom-water anoxia
92 to such an extent, that the system experiences a distinct increase in organic matter burial (Pilla et al.,
93 2020). Studies have also found catchment and basin structure to be important when considering the
94 extent to which sedimentary Hg signals reflect hydroclimate-driven variability, as both influence the
95 ease with which water is able to transport Hg to, from, and between discrete terrestrial sinks (Paine et
96 al., 2024).

97 ~~Earth's hydroclimate is highly variable in space and time (Bradley and Diaz, 2021).~~ In the short-term,
98 these interactions may manifest as annual changes in rainfall intensity and seasonality, or by sub-
99 decadal fluctuations in regional-scale climate modes (e.g., El-Nino Southern Oscillation, North Atlantic
100 Oscillation; Hernández et al., 2020). In the long-term, variability in the form of prolonged droughts
101 and/or pluvials may occur in response to global-scale atmospheric reorganization lasting centuries,
102 and changes in the planet's orbital configuration on timescales of many millennia (Bradley and Diaz,
103 2021). These wet-dry oscillations are important on a continental-scale. For example, periods of
104 extreme hydroclimate variability are known to have caused major changes in environmental
105 conditions across sub-Saharan Africa during the late Pleistocene, lasting for multiple millennia (e.g.,
106 Scholz et al., 2007).

107 Millennial-scale changes in hydroclimate may also affect the Hg cycle. Sediment cores extracted from
108 the Pacific and Atlantic oceans show low-amplitude Hg signals corresponding to orbital-scale ($>10^4$-
109 year) changes in precipitation and rates of sediment delivery to the ocean (e.g., Chede et al., 2022;
110 Fadina et al., 2019; Figueiredo et al., 2022; Zou et al., 2021), and a growing number of terrestrial
111 successions also show Hg fluctuations coeval with climate-driven changes in local precipitation, cloud
112 formation, and ice/permafrost extent (e.g., Guédron et al., 2018; Nalbant et al., 2023; Paine et al.,
113 2024; Pan et al., 2020; Pérez-Rodríguez et al., 2018). However, few terrestrial Hg records extend
114 beyond the present interglacial (>12 ka), and even fewer come from the low-latitudes where tropical

115 rainforest, grassland and desert biomes are highly sensitive to millennial-scale hydroclimate variability
116 (Bradley and Diaz, 2021; Schneider et al., 2023). Thus, our current understanding of Hg behaviour
117 may not fully account for the impact of major, long-term hydroclimate changes on Hg transformation
118 and transport through tropical environments (Obrist et al., 2018; Schneider et al., 2023), highlighting
119 the need for new Hg records spanning long (>10^3-year) timescales.

120

1.2.3 ~~West African Monsoon~~Research objectives

122 Sedimentary records offer an opportunity to assess the impact of millennial-scale hydroclimate
123 variability, and related effects, on the terrestrial Hg cycle. In ~~its domain,~~sub-Saharan Africa, the West
124 African Monsoon (WAM) regulates precipitation amount and distribution, and drives long-term
125 evolution of environmental characteristics and mineral-dust emissions (O'Mara et al., 2022; Kaboth-
126 Bahr et al., 2021; Kuechler et al., 2013; Weldeab et al., 2007). Proxy records from ~~sub-Saharan~~
127 ~~Africa~~this domain show that orbitally-driven variations in the strength of the WAM have frequently
128 driven ~~severe drought events~~distinct arid (Cohen et al., 2007; Scholz et al., 2007) and humid periods
129 (Armstrong et al., 2023; Menviel et al., 2021) throughout the Pleistocene. These humid and arid
130 periods have been linked to distinct changes in vegetation structure, ecosystem dynamics, and
131 human evolution across the continent (e.g., Cohen et al., 2022; Foerster et al., 2022; Gosling et al.,
132 2022b). In light of growing evidence for a hydroclimatic influence on the terrestrial Hg cycle (e.g.,
133 Guédron et al., 2018; Nalbant et al., 2023; Paine et al., 2024), we hypothesized that humid and/or arid
134 periods in sub-Saharan Africa would have elicited measurable changes in the Hg cycle, producing
135 measurable signals in regional sedimentary records. ~~This study focusses~~Here our focus is on
136 sediment core BOS04-5B extracted from Lake Bosumtwi, Ghana (West Africa): a core that~~, which~~
137 provides a clear and continuous record of this hydroclimate variability covering the late Pleistocene
138 (Koeberl et al., 2007).

139 Lake Bosumtwi is a closed system isolated from the regional groundwater network, rendering it
140 sensitive to both short and long-term variability in rainfall, humidity, and dynamic surface processes
141 (Shanahan et al., 2008b; Turner et al., 1996). Integrated proxy data shows that Lake Bosumtwi
142 experienced dramatic changes in water balance, aeolian dust inputs, and biological productivity
143 throughout its history. These changes all correspond to moisture-driven oscillations between a forest
144 and grass-dominated catchment in response to insolation-driven variability in WAM strength, and
145 migration of the Intertropical Convergence Zone (ITCZ) (Vinnepand et al., 2024; Gosling et al., 2022a;
146 Miller et al., 2016; Peck et al., 2004). Focussing on the uppermost ~47 m of the Lake Bosumtwi
147 sediment record, this study ~~aims to~~ assesses whether major shifts in local hydroclimate produced
148 measurable changes in how Hg has been transported to, and buried within, this system since ~96 ka.
149 By comparing our sedimentary Hg record with proxy data from archives across the African continent
150 (e.g., Foerster et al., 2022; Scholz et al., 2007), we explored whether hydroclimate has exerted a
151 measurable effect on terrestrial Hg cycling in the WAM domain in over the past ~100-kyr.

152

2. Site Description

2.1. Lake Bosumtwi

Lake Bosumtwi is the only natural lake in Ghana, West Africa (6°30' N, 1°25' W) (**Fig. 1**). It occupies a 1.08 ± 0.04 Ma meteorite impact crater dated to 1.08 ± 0.04 Ma, which is one of the youngest and best preserved impact craters on Earth (Jourdan et al., 2009). The surrounding bedrock and meteorite impact target rocks are Proterozoic metagraywackes, phyllites and metavolcanic rocks of the Birimian Supergroup (~2 Ga) (Jones et al., 1981). Lake beds, soils, and breccias constitute the most recent rock formations at the site, and are associated with evolution of the crater through time (Koerberl et al. 2007). excavated in metamorphosed and crystalline rocks of the Birimian Supergroup (~2 Ga). The present-day lake is ~8.5 km in diameter, with a water depth of up to 80 m at the lake centre, and the lake water level is currently at least 120 m below the crater rim (Shanahan et al., 2007). The crater itself is ~10.5 km in diameter at the rim with steep slopes, and a well-defined spillway (~120 m above the present lake surface) marks evidence of lake overflow likely during the most recent humid period (**Fig. 1**) (Shanahan et al., 2015). The lake is meromictic, with a shallow oxycline located ~10–15 m below the water's surface (Turner et al., 1996).

The Bosumtwi basin is hydrologically closed with no external drainages, connection to the regional groundwater aquifer, river or stream inflow originating outside of the crater (**Fig. 1**) (Turner et al., 1996). Only during exceptionally high lake levels does water leave the lake, through the spillway (Shanahan et al., 2007). Approximately 300 m of sediment has accumulated in the centre of the basin originating from biological processes within the lake, progressive erosion of the crater wall, aeolian transport, and vegetation within the crater (Koeberl et al., 2005). These properties render the lake highly sensitive to changes in atmospheric processes, but also imply that Hg inputs may originate exclusively from the atmosphere (e.g., by wet deposition). Therefore, this system is ideally suited for exploring whether specific basin characteristics (e.g., depth, nutrient status, bathymetry) could also measurably affect how Hg signals are encoded in the sedimentary record.

2.1.1. West African Climate

Seasonal variability in the tropical rain belt position drives short-term (<10-year) hydroclimate change in West Africa. During boreal summer, an increase in northern hemisphere summer (June to August) insolation triggers a northward ITCZ shift, creating a pressure gradient that brings moisture eastwards from the Atlantic Ocean to western Africa. The opposite occurs in boreal winter (December to February), where the ITCZ is displaced southwards, bringing dry, aerosol-rich, continental trade winds to West Africa. Together, these seasonal shifts produce distinct annual wet (May to October) and dry seasons.

On longer (>10^4-year) timescales, hydroclimate variability in West Africa has been linked to cyclic changes in Earth's orbital configuration. Changes in axial precession produce fluctuations in seasonal insolation above the African continent, influencing the strength of the WAM, the Walker Circulation,

190 the position and dimensions of the ITCZ, and the availability of continental moisture (Gosling et al.,
191 2022b; Kaboth-Bahr et al., 2021; Trauth et al., 2021). Several studies have shown weakening of the
192 WAM and southward migration of the ITCZ in response to high precession and/or changes in
193 insolation gradient, producing drier conditions in West Africa and subsequent reductions in terrestrial
194 precipitation, ecosystem productivity, and recession of terrestrial forests. ~~High precession causes~~
195 ~~weakening of the WAM and southward migration of the ITCZ, producing drier conditions in West~~
196 ~~Africa and subsequent reductions in terrestrial precipitation, ecosystem productivity, and recession of~~
197 ~~terrestrial forests (Menviel et al., 2021).~~ Conversely, strengthening of the WAM and a more northerly
198 ITCZ position is documented when precession is low, bringing wetter and warmer conditions to West
199 Africa and causing expansion of dense forests, voluminous lakes, and diverse ecosystems
200 (Larrasoaña et al., 2013; Pausata et al., 2020). During the last glacial cycle, moisture availability in
201 West Africa also fluctuated in conjunction with the waxing and waning of high-latitude ice sheets, and
202 their effects on sea-surface temperatures (SSTs) in the North Atlantic (deMenocal, 1995; Weldeab et
203 al., 2007). This teleconnection exists as a function of atmospheric moisture transport and convection
204 processes occurring in the polar and tropical regions. Low global ice volumes typically correspond to
205 warmer North Atlantic SSTs, driving increased atmospheric moisture transport and hence more moist
206 conditions in West Africa. Conversely, high global ice volumes generally correspond to cooler SSTs in
207 the North Atlantic, and subsequently drier conditions in West Africa (e.g., Crocker et al., 2022; Lupien
208 et al., 2023; Stager et al., 2011; Tjallingii et al., 2008).

209

2.1.2. Local hydrology and vegetation

211 Approximately 49% of the Bosumtwi drainage basin (area: 106 km^2) is currently occupied by the lake.
212 Situated in close proximity to the (current) ecological transition-zone between savannah in the north
213 and moist forest in the south, Lake Bosumtwi lies directly in the seasonal migration path of the ITCZ
214 (Nicholson, 2013). It experiences a current mean annual temperature of ~26°C, ranging between
215 ~23°C in August to ~27°C in February, with cooler summer temperatures attributed to increased
216 cloudiness and related reduction in incoming solar radiation (Shanahan et al., 2007). Present-day
217 humidity ranges from ~85% in August to ~75% in January, and average annual precipitation is ~1450
218 mm (Turner et al., 1996). At present, the surrounding catchment as classified as a '*Tropical and
219 Subtropical Moist Broadleaf Forest'* biome (White, 1983), meaning it is heavily forested with well-
220 developed tropical soils, although many flat-lying areas have been converted to agriculture (e.g.,
221 maize, plantain, cocoa, and oil palm) in recent decades (Boamah and Koeberl, 2007). Before human
222 occupation of the site, the lake was surrounded by a moist semideciduous forest, with a canopy
223 including abundant of trees from the Ulmaceae and Sterculiaceae (flowering plant) families (Miller and
224 Gosling, 2014).
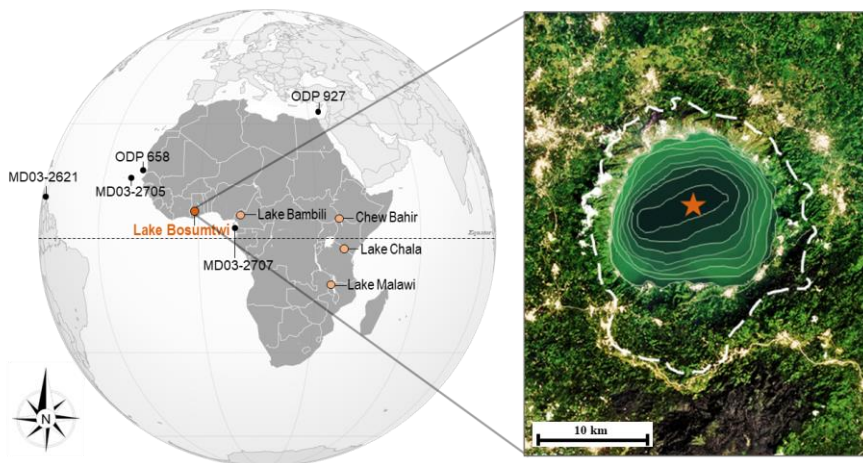
Figure 1: (Left) Location of key lake and marine sediment archives in and around Sub-Saharan Africa (SSA). (Right) An aerial photograph of Lake Bosumtwi (*copyright*: NASA, 2018), on which the location of the BOS04-5B drill site is marked as an orange star. Contours show lake bathymetry, with each step representing a 10 m depth change and culminating in a maximum depth of 75 m (Shanahan et al., 2012). The spillway notch is in the eastern rim of the crater, and the dashed white line marks the extent of the drainage divide (Brooks et al., 2005; Shanahan et al., 2006).

2.1.3. Paleoclimatic significance

Lake Bosumtwi provides an excellent record of millennial-scale hydroclimate change in West Africa. The upper ~47 m of sediment corresponds to the interval ~96 ka to present, and contains a series of distinct lithological features suggesting pronounced, climate-driven changes in lake level, catchment structure, and sediment transport processes (Vinnepand et al., 2024; Gosling et al., 2022a; McKay, 2012; Miller et al., 2016). For example, a massive, clastic-rich blue-grey clay unit is present between ~34 and 32 m depth, where TOC values drop to <1% and bulk density values increase by >60% (Scholz et al., 2007). Interpreted and referred to as Arid Interval(AI)-1 (McKay, 2012), this unit formed during extremely dry climatic conditions leading to near-total desiccation of the lake, and this interpretation is further supported by identification of a clear erosional unconformity corresponding to the age of the AI-1 unit in seismic reflection profiles (Brooks et al., 2005; Scholz et al., 2007).

Changing physical properties and geochemistry of sediments deposited prior to and following Unit AI-1 appear to reflect regional hydroclimate shifts (Scholz et al., 2007). Prior to AI-1, the presence of clastic-rich, organic-depleted sediments suggest a progressive reduction in water depth, likely in response to a (long-term) negative water balance (McKay, 2012; Shanahan et al., 2008b). Following AI-1, an abrupt reduction in clastic material concentrations, increased TOC, diagenetic carbonate, and lamination frequency all imply oxygen depletion at the sediment-water interface – evidence for a shift

243 to a positive water balance (McKay, 2012; Scholz et al., 2007; Shanahan et al., 2008a). The core also
244 shows distinct co-enrichment in manganese (Mn) and iron (Fe) in certain intervals following AI-1,
245 which that are associated with manganosiderite (Mn-rich $FeCO_3$) precipitation in the lake sediments.
246 Manganosiderite requires anoxic non-sulphidic (ferruginous) pore-water conditions and high dissolved
247 inorganic carbon concentrations to precipitate (Brumsack, 2006; Tribovillard et al., 2006), and
248 appears as a consequence of the redox tower migrating into the water column: a response to
249 increasing water column stratification, and overall lake level (Shanahan et al., 2006). The closed
250 hydrology of Lake Bosumtwi means that changing water levels are likely to reflect the magnitude of
251 precipitation variability in the region, with higher lake levels typically occurring during wetter climate
252 intervals (Russell et al., 2003; Shanahan et al., 2008b). However, lake level may have also been
253 influenced by secondary processes such as evaporation, and, over long time-scales, sediment infill
254 (McKay, 2012).

3. Material and methods

3.1. BOS04-5B

258 Core BOS04-5B was recovered in 2004 as part of the International Continental Drilling Program
259 (Koeberl et al., 2005) (full details in **S1**). Our study focuses on the upper ~47 m section of a 296-m-
260 long core extracted from deep-water (76 m) site 5 (core BOS04-5B; **Fig. 1**), which that extends from
261 the present-day lake floor to the brecciated bedrock dated by $^{40}Ar/^{39}Ar$ to 1.08±0.04 Ma (Jourdan et
262 al., 2009). Over ~67% of the full 294 m-long (~1-Myr) sediment succession is laminated (Koeberl et
263 al., 2007), with distinctive alternating clastic, organic and carbonate laminae (Shanahan et al., 2012,
264 2009, 2008a). Thicker laminations are visible either as packets of light grey microturbidites, or distinct
265 yellow and orange carbonates produced by enhanced redox-related precipitation of Fe and Mn
266 bearing minerals (Shanahan et al., 2008a).

267 After drilling in 2004, core BOS04-5B was shipped to the University of Rhode Island and split. The
268 physical properties of the full ~296 m core were measured at 2-cm intervals using a Geotek ® multi-
269 sensor core logger (Koeberl et al., 2007). After logging and imaging and at 4-cm resolution, 2 cm thick
270 slices were removed from the core half and separated into sub-samples for multi-proxy analyses,
271 including sediment magnetic hysteresis, x-ray diffraction mineralogy, total organic and inorganic
272 carbon content, bulk organic carbon and nitrogen isotopes, grain size, pollen, and charcoal (e.g.,
273 Gosling et al., 2022; McKay, 2012; Miller et al., 2016). Following bulk sediment analyses, the BOS04-
274 5B core material was transferred to the Continental Scientific Drilling (CSD) Repository in
275 Minneapolis.

3.2. Chronology

278   Age control for the ~47 m of sediment analysed in this study is provided by the BOSMORE7 model,

279   ~~generated~~ presented by Gosling et al. (2022). Using a combination of radiocarbon (calibrated ^{14}C; n=

280   109), optically stimulated luminescence (OSL; n=22) and uranium-thorium (U/Th; n=5) dates as

281   independent tie-points, Bayesian modelling suggests that the upper ~47 m of sedimentation at Lake

282   Bosumtwi corresponds to the interval ~96–0 ka (full details in **S3**) (Gosling et al., 2022a; Shanahan et

283   al., 2013). Age estimates for the AI-1 sedimentary unit are constrained by ^{14}C, OSL and U-Th dating

284   of the surrounding sediments, and suggest this unit formed between 77 and 71 (±5) ka (Scholz et al.,

285   2007; Shanahan et al., 2008b). The duration of the event is less clear due to the excessive erosion of

286   the newly exposed crater walls and reduction in distance between the shore and 5B core site (McKay,

287   2012) which may have led to unusually high sedimentation rates during this interval. Thus, slight

288   underestimation of sediment ages immediately following unit AI-1 may be expected.

289

290   3.3.   Sediment geochemistry

291   3.3.1.   Mercury

292   Total Hg (Hg$_T$) in the bulk sediments of core BOS04-5B was measured using the RA-915 Portable

293   Mercury Analyzer with PYRO-915+ Pyrolyzer, Lumex (Bin et al., 2001) at the University of Oxford. For

294   this study, we analysed 165 samples spanning the composite depth interval 47.7 to 0 m, with an

295   average temporal resolution of ~0.6 ka between each sample (range: 0.01 to 5.85 kyr). Dry powdered

296   sample material (45–100 mg) was heated to ~700°C, volatilizing Hg in the sample. Atomic absorption

297   spectrometry of the gases produced during pyrolysis quantifies the total Hg content of the sample. Six

298   different quantities of standard material (paint-contaminated soil – NIST Standard Reference Material

299   ® 2587) with a known Hg value of 290 ± 9 ng g^{-1} were ~~run~~ analysed to calibrate the instrument before

300   sample analysis, and then one standard for every 10 lacustrine samples **(supplementary data)**.

301   Calibration results accompany this article in a supplementary dataset. Long-term observations of

302   standard measurements *(n* = 390*)* for this instrument show average reproducibility (1 sigma) of 6% for

303   samples with ≥10 ng g^{-1} Hg (Frieling et al. 2023). Four (2%) of the analysed samples contained very

304   low Hg contents (<10 ng g^{-1}), and likely have uncertainties ≥10 %. Details of standard runs are

305   included as a supplementary file.

306

307   3.3.2.   Organic and inorganic carbon

308   Quantitative values for total organic carbon (TOC) and total inorganic carbon (TIC) content were

309   measured on the same powdered sample material also analysed for Hg, using a Strohlein Coulomat

310   702 (Jenkyns and Weedon, 2013) at the University of Oxford. Analytical reproducibility for this

311   instrument was ≤0.2 % based on repeat measurements, with a detection limit of ca. 0.1–0.2 %.

312   Powdered BOS04-5B sediment samples were split into two aliquots. Weights for aliquot 1 were

313   between 50–70 mg, and aliquot 2 between 90–120 mg. Prior to coulometric analysis, aliquot 2

314   samples were furnaced for 24 hours at 420°C in order to remove organic carbon fractions. Both

aliquots were then combusted in oxygen at 1220°C to break down the calcium carbonate and produce carbon dioxide (CO_2), ~~which~~ that was fed into a solution of barium perchlorate. By producing a change in solution pH from an initial value of 10.0, back titration to the original pH using electrolysis provided a measure of the amount of carbon originally present – quantified by the amount of electricity required to restore a pH of 10.0 and recorded in counts (Jenkyns, 1988; Jenkyns and Weedon, 2013). Counts obtained for aliquots 1 and 2 were used to calculate the total carbon (TC) content of each aliquot in wt.%, using the formula:

$$TC = \frac{total\ counts \times 0.2}{M} \quad \text{(eqn. 1)}$$

where M is the sample mass in mg.

TOC was calculated as follows:

$$TOC = TC_1 - TC_2 \quad \text{(eqn. 2)}$$

where TC_1 and TC_2 represent the TC values obtained for aliquots (1) and (2), respectively. TC_2 represents the TIC value for the sample.

3.3.3. Authigenic carbonates

The BOS04-5B succession contains variable amounts of diagenetic carbonates, predominantly (mangano-)siderite (**Fig. S2**) (McKay, 2012). Siderites commonly form in freshwater settings at shallow sediment depths under anaerobic (anoxic) conditions accompanied by organic-rich sediments (Armenteros, 2010; Sebag et al., 2018). However, they can also preclude accurate measurement of organic carbon content in lacustrine sediment via pyrolysis- or furnace-based methods, causing systematic overestimation of total organic carbon (TOC) due to the fact that thermal decomposition of siderite typically starts at temperatures <420°C (Sebag et al., 2018), which is lower than that which is used to remove the organic fraction on the Coulomat (Jenkyns, 1988). To assess whether siderite-associated carbon had an appreciable impact on the TOC measurements, we also analysed the carbon release from sixteen BOS04-5B samples spanning a range of low to high XRF-derived Mn counts (i.e., covering the possible range of (mangano-)siderite contents) using a weak acid (warm 5% HCl) treatment, following established methodologies (Brodie et al., 2011; Vindušková et al., 2019). Full details are provided in **S6**. Comparison of acid-treated and furnaced samples showed no systematic offset nor a clear correlation with the Mn counts from XRF data (**Fig. S2c**), suggesting that the carbon release from siderite did not appreciably bias TOC measurements.

3.3.4. Scanning X-Ray fluorescence

The Hg data for core BOS04-5B generated in this study are paired with unpublished x-ray fluorescence (XRF) data (McKay, 2012). The bulk elemental composition of the core was quantified

349 using the Itrax® scanning XRF analyser at the Large Lake Observatory at the University of
350 Minnesota. Core material was analysed at 1-cm-resolution with 60 sec count times, and a Mo X-ray
351 source run at 30 kV and 20 mA. Analytical and correctional procedures for element abundance
352 measurements covering the upper ~159 m (~500-kyr) of BOS04-5B are fully described in **S7**. To
353 mitigate any effects arising from changes in the physical properties of the BOS04-5B sediments (e.g.
354 compaction) and/or the measurement times, we applied a centred-log ratio (clr) transformation to the
355 measured XRF values. The centred log-ratio (clr) values are calculated by dividing the intensities of
356 an element by the average of the intensities obtained on all selected elements, and are dimensionless
357 such that positive values are generated for elements with high intensities, and vice versa (Bertrand et
358 al., 2024). Therefore, elements (X) subject to this transformation are presented as their centred-log
359 ratio value (X_{clr}).

360

3.4. Mercury normalization

362 It is common practice to assess both total Hg concentration (Hg_T) and normalised Hg (Hg/X) with the
363 aim to reduce, at least partially, the potential impact of variability in a dominant carrier/host phase (X)
364 on Hg_T (Sanei et al., 2012; Shen et al., 2020). Organic matter (here expressed as TOC) is commonly
365 considered the primary host phase of sedimentary Hg (Ravichandran, 2004). However, variability in
366 Hg_T may also be associated with variability in the abundance of detrital minerals, usually detected by
367 a correlation between Hg and detrital elements such as Al or K (Paine et al., 2024; Them et al., 2019),
368 and very rarely in sulphate-limited (lacustrine) sediments, sulphides (Benoit et al., 1999; Han et al.,
369 2008). Exploration of Hg signal variability relative to distinct shifts in the abundance, contribution
370 and/or sources of host phases can therefore elucidate the timing and magnitude of shifts in lake
371 hydrology, sedimentation regime, and geochemistry, and whether these are connected to changes in
372 the Hg cycle or sediment composition changes (Paine et al., 2024).

373 To isolate the effects of local depositional and/or transport processes on Hg signals recorded in the
374 sediments of Lake Bosumtwi, we normalised Hg_T values to organic matter (TOC) and detrital mineral
375 abundance estimated from potassium (K) intensities; with the assumption that the strongest positive-
376 sloped linear correlation with Hg_T among these elements signals the most likely dominant impact of
377 host phase variability in that section of the core. To account for differences in resolution between Hg
378 and XRF data, K measurements were averaged to obtain a K value corresponding to the interval
379 covered by each discrete Hg sample (~0.5 cm thickness).

380

3.5. Mercury accumulation

382 The total Hg mass accumulation rate (Hg_{AR}) in core BOS04-5B was calculated from:

383 $$Hg_{AR} = Hg_T \, (DBD \times SR) \qquad \text{(eqn. 3)}$$

384 where Hg_{AR} is in mg m^{-2} kyr^{-1}, Hg_T is the total mercury concentration (mg g^{-1}), DBD is the dry bulk

385 density (g m^{-3}), and SR is the sediment accumulation rate (m kyr^{-1}). Values for Hg_{AR} are also

386 calculated with respect to the median age estimate for each sample. We do not present maximum

387 and minimum Hg_{AR} values here, but note that uncertainties increase with depth due to increasing

388 uncertainties in sedimentation rates, which are calculated based on the BOSMORE7 age model and

389 average ~0.08 cm yr^{-1} (0.02–0.3 cm yr^{-1}).

390 DBD values were calculated using measurements obtained by loss-on-ignition (McKay, 2012;

391 Shanahan et al., 2013), using the formula:

392 $$DBD = M_{solid}/V_{total} \qquad \text{(eqn. 4)}$$

393 where M_{solid} is the mass of dry solid material (g) in each sample, and V_{total} is the volume of each

394 respective sample (0.5 cm^3). To calculate M_{solid}, the proportion of clastic material was multiplied by an

395 assumed grain density value (2.6 g cm^{-3}) representative of a mixture of common sedimentary

396 minerals (e.g. quartz, clay minerals, clastic; typically range of 2.6 to 3 g cm^{-3}) and the total volume.

397 The proportion of clastic material was calculated by first accounting for the proportion of water and

398 organic matter (measured by McKay (2012) and Shanahan et al. (2013) in each sample and

399 assuming the residual was all clastic material. DBD values generally increase with core depth, which

400 reflects the impact of increasing sediment compaction and dewatering with age (Shanahan et al.,

401 2013). Calculated values of DBD average 1.15 g cm^{-3}, which is broadly consistent with measurements

402 taken from other African lake sediment successions of similar age (<100 ka), composition (silty clays

403 between 0.6–1.1 g cm^{-3}), and structure (high porosity) (e.g., Cohen et al., 2016; Scholz et al., 2007).

3.6.   Statistical analyses

405 Two statistical analyses were used in order to more quantitatively explore the timing, and expression

406 of signals recorded in the BOS04-5B Hg_T dataset. First was a simple linear Pearson's correlation

407 analysis, from which correlation coefficients (r) were calculated to indicate the direction and strength

408 of the association between Hg (n = 157), and a suite of geochemical proxies also measured in the

409 core. Second was a change point analysis, to determine whether distinct changes in mean values of

410 Hg_T occur within the record using PAST v.4.16 software (Hammer et al. 2001). This software employs

411 a Bayesian Markov chain Monte Carlo (MCMC) approach, which was run on default settings with a

412 total of 1 million MCMC simulations were run for each test and a maximum of ≤10 changepoints. The

413 extent to which similar processes influenced the concentration of Hg_T, TOC, K, and detrital matter

414 were also explored, and correlations were subdivided based on visual examination of the Hg_T records

415 (and supported by changepoint analyses). The significance of all correlations was assessed using a

416 Student's t-test, which showed that ~50% of the assessed geochemical combinations were significant

417 at p<0.01.

419 # 4. Results

Core BOS04-5B from Lake Bosumtwi shows distinct fluctuations in total sedimentary Hg concentration (Hg$_T$) throughout the ~47 m succession. Values range from 10 to 370 ng g^{-1} (median: 58 ng g^{-1}) (**Fig. 2**). The Hg$_T$ curve broadly tracks that of TOC, which shows similarly pronounced variability ranging between 0.1 to 23 wt. % (median: 6.5 wt. %) (**Fig. 2**), and peaking between 5.2 and 3 m depth. Calculated Hg accumulation rates (Hg$_{AR}$) do not follow the same pattern as Hg$_T$ and TOC. Ranging between 2.9 and 460 mg m^{-2} kyr^{-1}, calculated values instead broadly track the sedimentation rate curve presented in **Figure 2**. Large peaks in Hg$_{AR}$ are visible between 8 and 6 m depth and then again between 2 and 0 m, and these Hg$_{AR}$ peaks are both coeval with reductions in TOC below ~10 wt.%. The lowest Hg$_{AR}$ values are recorded in the lower core section between ~47 and 34 m depth.
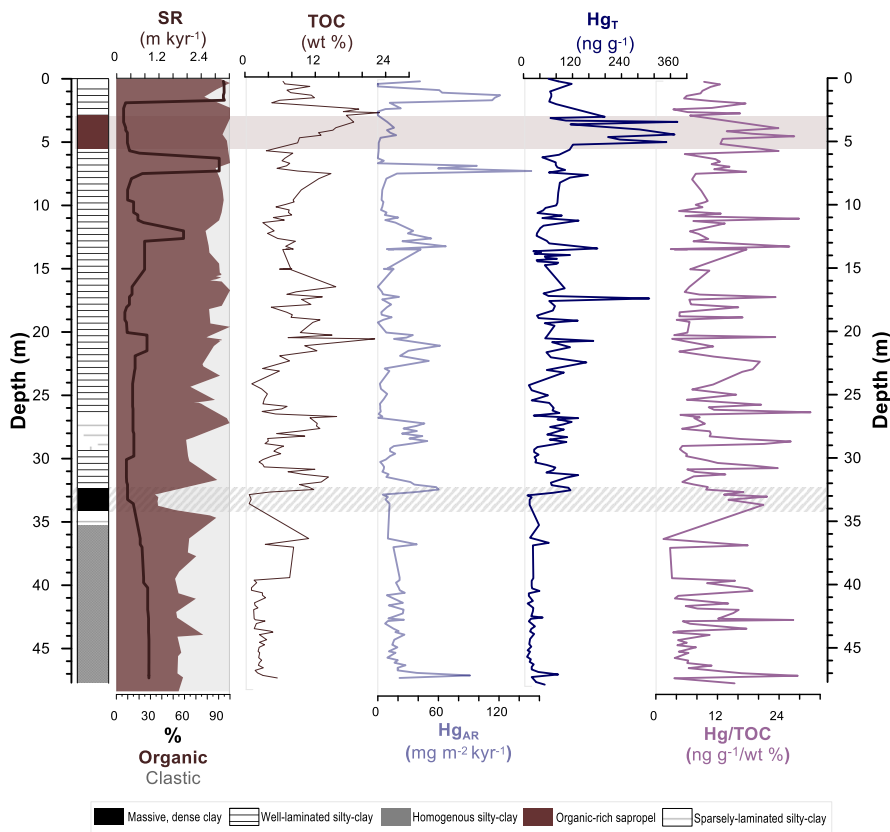
Figure 2: Depth-resolved profiles of total organic carbon (TOC), total Hg (Hg$_T$) and Hg accumulation rate (Hg$_{AR}$) profiles obtained for core BOS04-5B from Lake Bosumtwi in this study, relative to key lithofacies and sedimentological data including records of sedimentation rate (SR; *this study*), and the proportion of biogenic to terrigenous material (% organic) within the core (McKay, 2012). A distinct lake low stand referred to as Arid Interval 1 (AI-1) based on seismic profiles and sedimentological data is marked between 33.5 and 32.8 m depth (grey dashed shading; McKay, 2012; Scholz et al., 2007). Limited samples were available between ~39 and 34 m depth

(**Fig. S1**). Sapropel layer Unit S1 is marked between 3–5.5 m depth (brown shading; Russell et al., 2003; Shanahan et al., 2008a; Talbot and Johannessen, 1992). We also present ratios of Hg_T to TOC, following evidence for a positive correlation between the two compounds ($r^2 = 0.42$) (see **section 5.1**).

429

430   Changing Hg signals in Lake Bosumtwi correspond to measurable changes in lake sedimentation.
431   From ~47 to 32 m depth, low amplitude, muted variability in both Hg_T and Hg_{AR} corresponds to a
432   homogeneous sequence of silty-clay sized material generally depleted in TOC, S, and high in detrital
433   materials. No clear changes in Hg_T nor Hg_{AR} are visible during AI-1 (34 – 32 m core depth), however,
434   variability in Hg concentration increases immediately following this interval. From ~32 m to the core
435   top, sediments show a progressive increase in Hg_T punctuated by several clear peaks, and more
436   pronounced fluctuations in Hg_{AR} (**Fig. 2**). This shift in Hg behaviour tracks a broad increase in the
437   organic content of the core compared to clastic, reflected by increasing TOC and decreasing K
438   profiles (**Fig. 2**). The clearest expression of this correspondence is seen between 5.2 and 3 m,
439   whereby the highest Hg_T values correspond to the organic-rich sapropel Unit S1.

440   Studying time-resolved changes in lake sediment Hg concentration provides a valuable opportunity to
441   study changes in the pre-industrial Hg cycle, how these changes translate to measurable sedimentary
442   signals, and their links to local and regional-scale environmental variability (Cooke et al., 2020). Two
443   mechanisms emerge as plausible drivers of Hg variability in Lake Bosumtwi (**Fig. 2**). First is external
444   changes in net Hg input to the system, and second is organic matter (host) availability.

445   ## ~~Discussion~~

446   ~~Studying time-resolved changes in lake sediment Hg concentration provides a valuable opportunity to~~
447   ~~study changes in the pre-industrial Hg cycle, how these changes translate to measurable sedimentary~~
448   ~~signals, and their links to local and regional-scale environmental variability (Cooke et al., 2020). From~~
449   ~~the data presented in **Figure 2**, two mechanisms emerge as plausible drivers of Hg variability in Lake~~
450   ~~Bosumtwi. First is external changes in net Hg input to the system, and second is organic matter (host)~~
451   ~~availability. Both are explored in the discussion below.~~

452

453   ### 4.1.   Lacustrine host phases of mercury

454   An overall positive association between Hg_T and TOC ($r = 0.64$; $r^2 = 0.42$) suggests that Hg variability
455   may be associated with organic carbon variability in Lake Bosumtwi. However, it is noteworthy that
456   detrital materials (e.g., K_{clr}) show negative correlations with both TOC ($r = -0.59$; $r^2 = 0.34$) and Hg ($r =$
457   -0.57; $r^2 = 0.32$) so that the Hg-TOC correlation may reflect, in part, a correlation imposed by variable
458   clay-dilution of both Hg and TOC. ~~An overall positive association between Hg_T and TOC ($r^2 = 0.42$)~~
459   ~~suggests that Hg variability may be associated with organic carbon variability in Lake Bosumtwi.~~
460   ~~However, it is noteworthy that detrital materials (e.g., K; $r^2 = 0.34$) show negative correlations with~~
461   ~~TOC and Hg (Fig. 3b) so that the Hg-TOC correlation may reflect, in part, a correlation imposed by~~
462   ~~variable clay-dilution of both Hg and TOC.~~ The broad statistical link between Hg and TOC is

supported by evidence for large Hg_T and Hg_{AR} peaks in core sections containing high TOC concentrations, most markedly in the upper sections (**Fig. 2**), and the relationship between Hg_T and TOC also strengthens following deposition of AI-1 (**Fig. 3a, S3**). However, the highest Hg_T values are not always recorded in the most TOC-enriched sediments, nor are TOC-depleted sediments also depleted in Hg_T (**Fig. 2**). Dilution of Hg by organic matter is unlikely to be the cause (Machado et al., 2016), nor can shift from an organic to detrital-dominated host-phase regime account for these signals, given that intervals characterised by an overall negative Hg and TOC correlation are coeval with similarly negative values for Hg and K_{clr} (**Fig. S3**). More likely is that they reflect changes in net Hg flux to the system, and hence the amount of Hg being supplied to (and sequestered in) Lake Bosumtwi.

A negative overall correlation between Hg_T and K_{clr} is apparent throughout the record (r = -0.57; r^2 = 0.32; **Fig. 3b**). A negative overall correlation between Hg_T and K is apparent throughout the record (r^2 = 0.34; **Fig. 3a**). Other robust proxies for the proportion of detrital and autochthonous components in biogenic-rich sediments include Fe, Ti, Rb, and Al (Grygar et al., 2019). Strong correlations between K_{clr} K and these detrital elements confirm this is likely also the case in Lake Bosumtwi (**Fig. 3b**), with enrichment of detrital materials in this core reflecting enhanced erosion and sediment transport to the BOS04-5B drill site (McKay, 2012; Shanahan et al., 2012). Moreover, the significant negative correlations between TOC, Hg_T, and all elements associated with detrital components (K_{clr}, Ti_{clr}, Rb_{clr}, and Al_{clr}) (K, Ti, Rb, and Al) (**Fig. 3b**) suggest that detrital matter did exert a control on Hg_T. However, instead of increasing Hg, the negative correlation with detrital material suggests that 'Hg-depleted' detrital materials diluted the concentration of both Hg and its suggested host (TOC). Variations in both the detrital and Hg flux may also explain the somewhat counterintuitive decoupling of Hg_T and Hg_{AR} in some intervals, for example, between ~10 and 6 m depth (**Fig. 2**). Dilution-driven alteration of the sedimentary Hg record may be a common feature for depositional systems where supply of Hg is ultimately limited by atmospheric inputs (e.g., Chede et al., 2022).

Strong correlations between Hg_T and Mn_{clr}, and Hg_T and Fe_{clr} (redox sensitive elements) are also absent in BOS04-5B (**Fig. 3**). The majority of the examined record is marked by the presence of laminations, suggesting anoxic conditions dominate throughout (Shanahan et al. 2008). Although this means that redox changes were likely subtle, the coeval presence of siderite has potential implications for Hg through, for example, it's influence on Hg reduction (e.g., Ha et al. 2017). Fe is a major component of siderite, but it is also an important component of the detrital material that washes into Lake Bosumtwi and also potentially other redox-sensitive minerals precipitated in the lake and sediment pore waters (Shanahan 2006; Shanahan et al., 2008; 2009). In this record, we therefore test the relation between Hg_T and Mn peaks. Pronounced Mn enrichments signal periods of (mangano)siderite formation, and this constitutes the clearest indicator of (subtle) pore water redox changes (McKay, 2012; Shanahan et al., 2008). Moreover, siderite specifically may be involved in Hg cycling through its potential to reduce Hg (e.g., Ha et al. 2017). Overall, the lack of evidence for substantial redox changes from ubiquitous laminations and the absence of a strong correlation

501 between Mn and Hg$_T$ suggests that Hg concentrations in Lake Bosumtwi were not appreciably
502 influenced by changes in redox conditions, nor the diagenetic effects signalled by these elements.

503 Clear correlations between Hg$_T$ and Mn, and Hg$_T$ and Fe (redox sensitive elements) are also absent in
504 this record (**Fig. S4**), suggesting that Hg concentrations in Lake Bosumtwi was not appreciably
505 influenced by changes in redox conditions or diagenetic effects signalled by these elements.

506
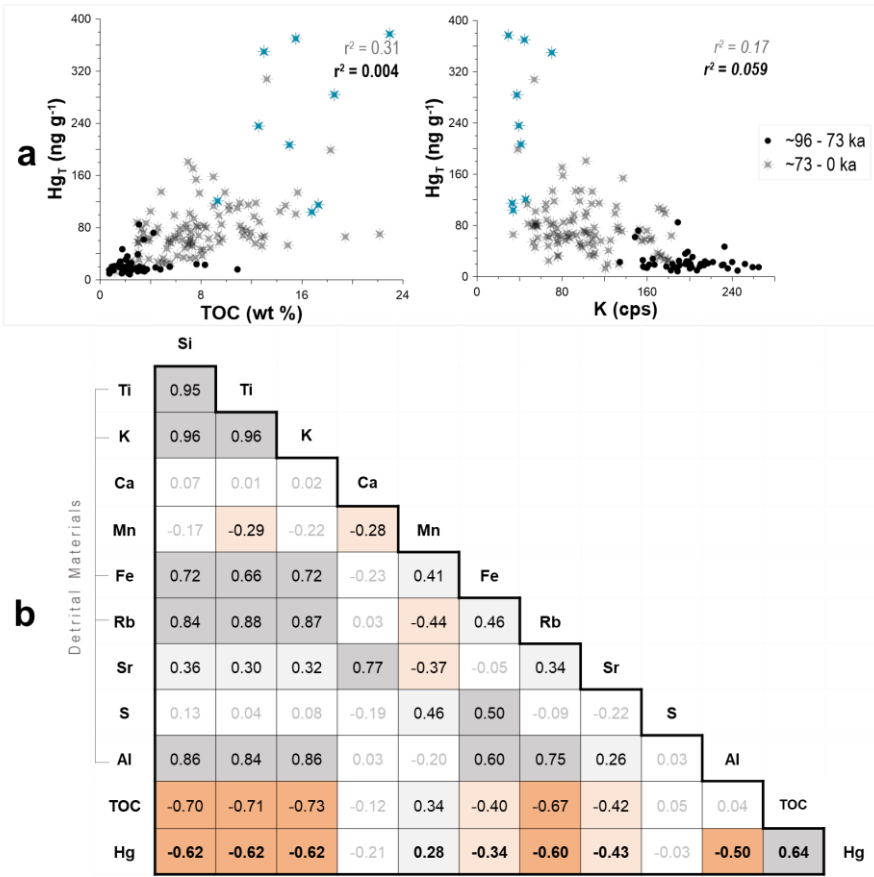
Figure 3: (a) Comparison of host-phase relationships in Lake Bosumtwi between ~96 and 73 ka (black
circles), and between ~73 and 0 ka (stars). We assess the Hg$_T$ record for this lake relative to total organic
carbon (TOC) values measured in this study, and detrital minerals (estimated by potassium (K))
concentrations measured by McKay (2012). R-squared (r^2) values for each interval are also given, with italic
formatting indicating a negative relationship. Stars marked in teal correspond to deposition of sapropel unit 1
(S1) in BOS04-5B. **(b)** Full-core correlation (Pearson's r) matrix for Hg, total organic carbon (TOC) (this study),
and a suite of trace elements measured in BOS04-5B by XRF (McKay, 2012 Higher r values suggest that

Formatted Table

Figure 3: (a) Full-core correlation (Pearson's r) matrix for Hg, total organic carbon (TOC) (this study), and a suite of clr-transformed XRF data measured in BOS04-5B by XRF (McKay, 2012). Higher r values suggest that similar processes influence the concentration of the two elements in focus). Sample size (n) was 157 for each analysis, and >50% of the assessed trace element combinations were significant (p<0.01). Those combinations that were not are marked with an asterisk (*). Grey shading marks positive correlations (light: >0.25, dark: >0.5), and orange shading marks negative correlations (light: <-0.25, dark: <-0.5). Unshaded boxes mark weak/negligible correlations (between 0 and 0.25, and 0 and -0.25), with values greyed-out for clarity. All remaining values are presented with black text, with those in this range related to Hg in the boldest type. **(b)** Comparison of relationships in Lake Bosumtwi between ~96 and 73 ka (black circles), and between

~73 and 0 ka (stars). We first assess the Hg$_T$ record for this lake relative to two potential host-phases: total organic carbon (TOC) values measured in this study, and detrital minerals (estimated by potassium (K)) concentrations measured by McKay (2012). We also test the relationship between Hg$_T$ and first principal component (PC1) of the BOS04-5B XRF data, in which 39% of total variance is strongly associated with terrigenous elements, and so interpreted as an indicator of lake level changes (McKay, 2012). R (r) and r-squared (r^2) values for each interval are also given, n = 157 for each plot. The significance of all correlations were assessed using a Student's t-test, which showed that all three combinations were significant at p<0.01 Stars marked in teal correspond to deposition of sapropel unit 1 (S1) in BOS04-5B.

5. Discussion

4.2.5.1.   Environmental drivers

Time resolved Hg$_T$ and Hg$_{AR}$ profiles generated from the sediments of Lake Bosumtwi show two broad periods of differing Hg behaviour: (1) ~96 – 73 ka (low Hg$_T$ and Hg$_{AR}$) and (2) ~73 – 0 ka (moderate/high Hg$_T$, and large fluctuations in Hg$_T$ and Hg$_{AR}$) (**Fig. 4**). Each corresponds to different lake level evolution trends with broadly decreasing lake level between ~96 and 73 ka (although with a substantial rise between 95 and 80 ka), and rising from ~73 to 0 ka (**Fig. 4**). Lake Bosumtwi's hydrology is controlled by a balance between direct precipitation and runoff with water removal limited almost entirely to evaporation; exceptions being rare transient overspilling events (Turner et al., 1996). Taking this unique hydrology into account, our discussion below explores how different environmental processes relate to changes in Hg behaviour during these two discrete intervals, and how the significance of these processes may have changed through time.
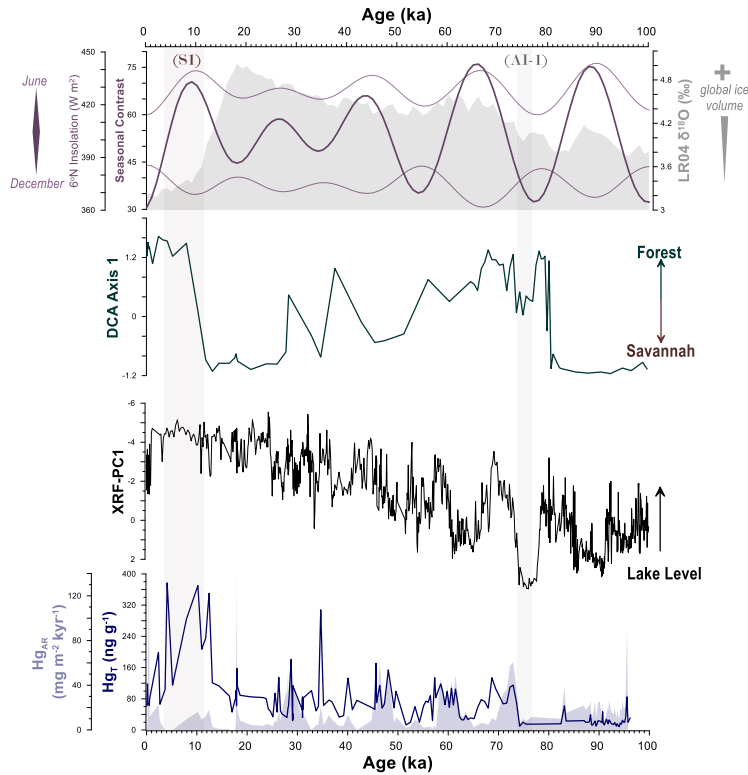
Figure 4: Comparison of key proxy datasets. Included are (from bottom to top), total mercury (Hg$_T$) and mercury accumulation rate (Hg$_{AR}$) for Lake Bosumtwi from this study, chosen as the most appropriate proxies for Hg variability in this core (see **section 5.1**). The first principal component (PC1) of the BOS04-5B XRF data (39% of total variance) is strongly associated with terrigenous elements, and so interpreted as an indicator of lake level changes (McKay, 2012). Forest (woody) taxa abundance (presented as DCA Axis 1; Gosling et al., 2022a; Miller et al., 2016). Lack of data for woody taxa presence is assumed to imply a savannah-dominated regional landscape. Insolation at 6°N (location of Lake Bosumtwi) in June (summer) and December (winter) are calculated following the astronomical solution presented by Laskar et al. (2004) (accessed via https://vo.imcce.fr/insola/earth/online/earth/online/index.php), and used to calculate seasonal insolation contrast at the Bosumtwi site since ~100 ka. Also shown is a record of benthic foraminiferal calcite δ^{18}O (‰) derived from the LR04 global stack) as a proxy for ice volume, with cold glacial stages defined by high δ^{18}O ratios (Lisiecki and Raymo, 2005a). Proxy data are all presented on the BOSMORE7 chronology. Unit AI-1 is marked between 33.5 and 32.8 m depth (grey shading; Brooks et al., 2005; Scholz et al., 2007), and sapropel layer Unit S1 is marked between 3–5.5 m depth (brown shading; Shanahan et al., 2012, 2006).
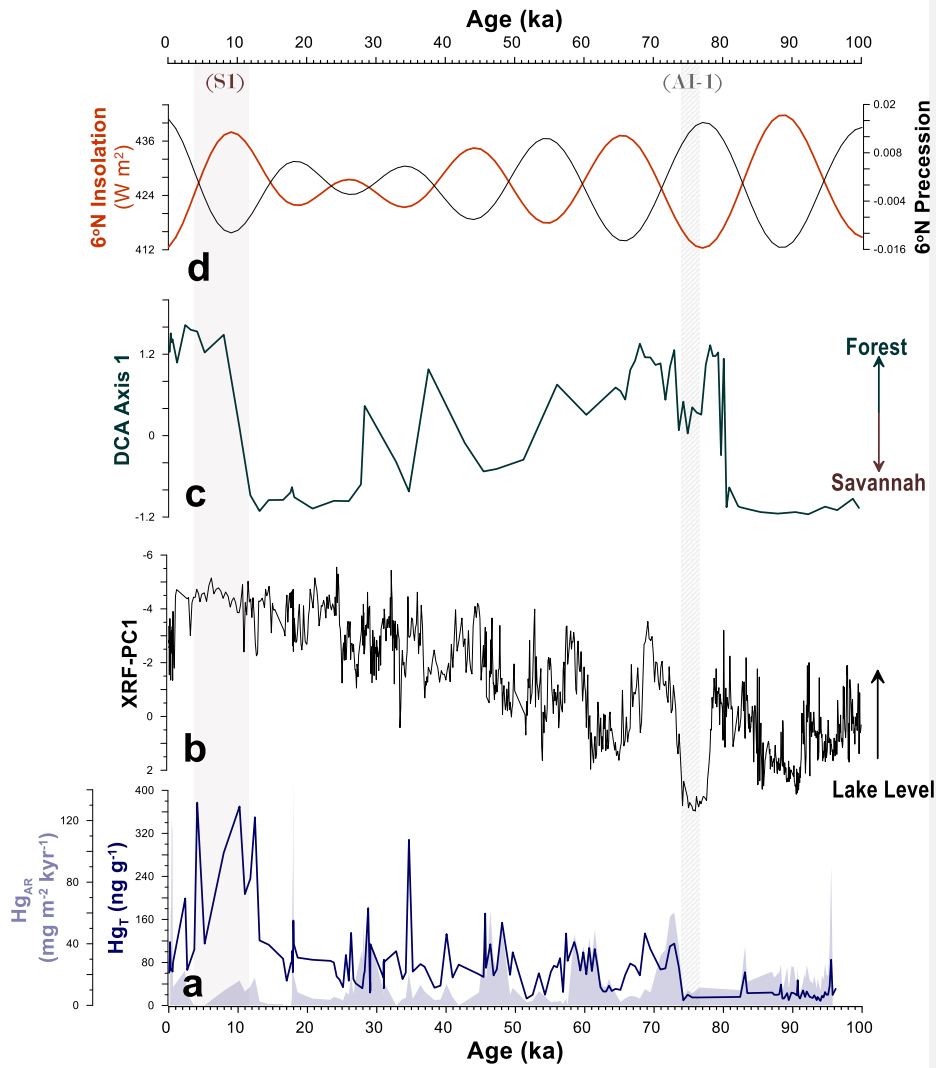
Figure 4: Comparison of key proxy datasets. **(a)** Total mercury (Hg_T) and mercury accumulation rate (Hg_{AR}) for Lake Bosumtwi from this study, chosen as the most appropriate proxies for Hg variability in this core (see **section 5.1**). **(b)** The first principal component (PC1) of the BOS04-5B XRF data (30% of total variance) is strongly associated with terrigenous elements, and so interpreted as an indicator of lake level changes (McKay, 2012). **(c)** Forest (woody) taxa abundance (presented as DCA Axis 1; Gosling et al., 2022a; Miller et al., 2016). Lack of data for woody taxa presence is assumed to imply a savannah-dominated regional landscape. **(d)** Annual mean insolation and precessional variability at 6°N latitude, calculated following the astronomical solution presented by Laskar et al. (2004) (accessed via. https://vo.imcce.fr/insola/earth/online/earth/online/index.php). Orbital precession

4.2.1.5.1.1.   Arid conditions (~96 to 73 ka)

Both Hg_T and Hg_{AR} show muted variability between ~96 and 73 ka (**Fig. 4a**). The presence of more clastic-rich/organic-depleted sediment (**Fig. 4b**), and reductions in tree pollen are both typical of a savannah-dominant, more open landscape (**Fig. 4c**), and so suggest generally arid conditions within the lake and its catchment prior to ~73 ka. These conditions would favour pronounced reductions in lake level (McKay, 2012; Miller et al., 2016; Scholz et al., 2007), and are consistent with a 24 – 38% reduction in local rainfall as estimated by water balance modelling) (Shanahan et al., 2008b). Reductions in lake level could facilitate an increase in water column vertical mixing, ventilation of bottom waters, more efficient breakdown of organic matter, and simultaneous sediment dilution by a sudden increase in eroded material fluxes (McKay, 2012; Scholz et al., 2007; Shanahan et al., 2012) – all of which could lead to a reduction in organic matter (host-phase) concentration. Indeed, several meromictic lakes have shown reduced organic matter content as a function of better ventilation and lower productivity during 'shallow' conditions (Katsev et al., 2010; Schultze et al., 2017), and new evidence suggests that changes in organic matter oxidation may produce comparably distinct changes in Hg sequestration (Tisserand et al., 2022).

The absence of a clear change in Hg_{AR} between ~96 and 73 ka might also reflect changes in the balances of Hg cycling in the lake. Lake Bosumtwi is a hydrologically closed system that receives >80% of its water from rainfall directly on the surface, meaning its hydrology and sedimentation regime is extremely sensitive to variability in precipitation and precipitation-evaporation balance (Shanahan et al., 2007; Turner et al., 1996). Thus, low Hg_T and Hg_{AR} values may reflect a reduction in wet deposition of atmospheric Hg at the Lake Bosumtwi site by precipitation, while Hg evasion back to the atmosphere remains high due to evaporation in the consistently warm, tropical temperatures (Schneider et al., 2023). Depletion of sedimentary Hg during drier climate intervals are documented in several other late Quaternary-age records, where they are interpreted as signs of a net reduction in Hg input relative to loss/evasion (e.g., Hermanns and Biester, 2013; Pompeani et al., 2018; Schneider et al., 2020; Schütze et al., 2021, 2018).

Desiccation of Lake Bosumtwi between ~75 and 73 ka (AI-1) corresponds to evidence for severe depletion of organic matter, and enrichment of detrital materials within the sediments (**Fig. 2**). Although a detailed characterization of local soil and bedrock Hg contents is currently lacking for Lake Bosumtwi, these changes in sediment composition (lower TOC, higher K) and low overall sedimentation rates are unaccompanied by coeval changes in Hg_{AR} (**Fig. 2**). In certain cases, one

would typically expect that the near-complete desiccation of a steep-sided lake would 'focus' trace metals (including Hg) at the central coring site, particularly during lake recessions following erosion of exposures around the crater rim (Blais and Kalff, 1995; Engstrom and Rose, 2013). However, evidence for low Hg burial both prior to and during AI-1 in Lake Bosumtwi suggests that over multiple millennia, changes in Hg supply to the BOS04-5B drill site were predominantly driven by atmospheric inputs, with minimal contribution from catchment-sourced materials.

4.2.2.5.1.2. Humid conditions (~73 to 0 ka)

The magnitude and frequency of variability in Hg_T visibly increases at ~73 (±5) ka (**Fig. 4**). The quantitative significance of this shift is supported by changepoint analysis of the BOS04-5B dataset, which demonstrates a clear and step-wise shift in mean Hg_T values between ~75 and 73 ka (Fig. S3). It also occurs in conjunction with an increase in the lake's water level (**Fig. 4b**). The magnitude and frequency of variability in Hg_T and Hg_{AR} increases at ~73 (±5) ka. This shift is coeval with an increase in the lake's water level (**Fig. 4b**), and . Furthermore, changing sedimentary TOC, terrigenous material, and pollen concentrations all corroborate a broad increase in local moisture availability, temperature, and humidity following deposition of the AI-1 unit (**Fig. 4**): a signal that coincides with the transition into the warmer Holocene interglacial, marked by reduced global ice volume and increased sea surface temperatures in the North Atlantic (McKay, 2012; Scholz et al., 2007; Shanahan et al., 2008b). Our data also shows a simultaneous increase in Hg_T, Hg_{AR}, and a decrease in detrital material concentrations following ~73 ka (**Fig. 4b, S5**), suggesting that Hg supply temporarily exceeded the diluting effects of clastic materials following lake level rise.

Lake deepening generally increases water column stratification, limiting the effects of vertical transport processes such as turbulent energy generated by surface winds and currents (Gulati et al., 2017). Deeper, more anoxic conditions are therefore typically associated with more effective organic carbon burial (Gulati et al., 2017; Schultze et al., 2017), coupled with more distinct formation of distinct laminations (Zolitschka et al., 2015) and precipitation of authigenic carbonates such as siderites (Swart, 2015). Given that elevated Hg_T and Hg_{AR} correlate most closely with TOC enrichment in Lake Bosumtwi following ~73 ka (**Fig. 3a**), this could suggest that Hg drawdown was moderated by an increase in organic matter availability and preservation, as an indirect function of bottom water deoxygenation. Evidence for an inverse relationship between sedimentary Hg concentration and hypolimnion oxygen content has been identified in a number of meromictic lake systems across the world (e.g., Schultze et al., 2017; Tisserand et al., 2022), and provides further support for our interpretation.

Geochemical evidence suggests sedimentary oxygen depletion became progressively greater in Lake Bosumtwi following ~73 ka, culminating with sapropel formation between 12.4 and 3.7 ka. This unit contains clear Hg_T enrichments relative to the rest of the core (**Fig. 2, 4a, S3**), is extremely rich in organic matter (~15-20%), and contains a high concentration of blue-green algae *Anabaena* deposits (Russell et al., 2003). Sapropelic layers have emerged as key sites of Hg enrichment from a suite of

588 marine and lacustrine-based studies, which suggest this may be due to changes in productivity,
589 sediment oxygenation, and diagenetic processes (e.g., Frieling et al., 2023; Gehrke et al., 2009; Jeon
590 et al., 2020). Scavenging of Hg from the water column by algae is also a process now recognised as
591 an important driver of Hg export to lacustrine sediments; particularly in systems where primary
592 productivity, organic matter production, and burial capacity is high (Outridge et al., 2007; Biester et al.,
593 2018; Schütze et al., 2021). These conditions are met in Lake Bosumtwi following ~73 ka, meaning
594 the observed changes in sedimentary Hg$_T$ could be linked to elevated rates of scavenging, as a
595 function of enhanced primary productivity.

596 In closed-basin lakes where fluxes of organic material from the catchment (e.g., soils and vegetation)
597 are minimal, measurable changes in sedimentary Hg concentration would require a simultaneous
598 increase in Hg fluxes to the system: to counterbalance Hg depletion by scavenging, methylation, or
599 evasion back to the atmosphere (e.g., Bravo et al., 2017; Hermanns et al., 2013; Outridge et al.,
600 2007; Schütze et al., 2021). For Lake Bosumtwi, these direct inputs may have come from
601 precipitation, and/or from increased flux of charcoal into the lake following local wildfire events (Cooke
602 et al., 2020).

603 Lake Bosumtwi records evidence for an increase in local precipitation following ~73 ka. Model and
604 proxy-based data show that the precipitation-evaporation balance is directly coupled to lake level in
605 this system, such that lake deepening occurs as a function of more rainfall (Shanahan et al., 2008b).
606 Proxy data generated from the BOS04-5B core suggest that progressively wetter conditions affected
607 the catchment following ~73 ka (e.g., Gosling et al., 2022a; Shanahan et al., 2008b). Paleoclimate
608 records based on the sediments of lakes Malawi (Tanzania), Bambili (Cameroon), Tanganyika
609 (Tanzania/Democratic Republic of the Congo), Chew Bahir (Ethiopia) and Chala (Tanzania) (e.g.,
610 Cohen et al., 2007; Foerster et al., 2022; Lézine et al., 2019; Scholz et al., 2007), and marine
611 sediment core material from the West African margin (**Figs. 1, 5**) (e.g., Kinsley et al., 2022;
612 Skonieczny et al., 2019) also pertain to a distinct regional-scale shift in hydro climate across tropical
613 sub-Saharan Africa (**Fig. 5**). Specifically, a shift characterized by a distinct
614 moisture gradient favouring wetter conditions in the west of the continent relative to the east, which
615 was further amplified during the last glacial termination (e.g., Baxter et al., 2023; Gosling et al., 2022a;
616 Lupien et al., 2023). , and were produced by a broader, regional-scale shift in hydroclimate across
617 sub-Saharan Africa (**Fig. 5**). These records include deep drill cores from lakes Malawi (Tanzania),
618 Bambili (Cameroon), Tanganyika (Tanzania/Democratic Republic of the Congo), Chew Bahir
619 (Ethiopia) and Chala (Tanzania) (e.g., Cohen et al., 2007; Foerster et al., 2022; Lézine et al., 2019;
620 Scholz et al., 2007), and marine cores extracted from the West African margin (**Figs. 1, 5**) (e.g.,
621 Kinsley et al., 2022; Skonieczny et al., 2019). Therefore, a coeval increase in the frequency and
622 amplitude of Hg enrichment in Lake Bosumtwi, and associated rise in lake level, could indirectly
623 reflect a regional-scalepronounced shifts in hydroclimate favouring wetter conditions in Westacross
624 tropical sub-Saharan Africa.

Formatted: French (Switzerland)
Field Code Changed
Formatted: French (Switzerland)
Field Code Changed
Field Code Changed
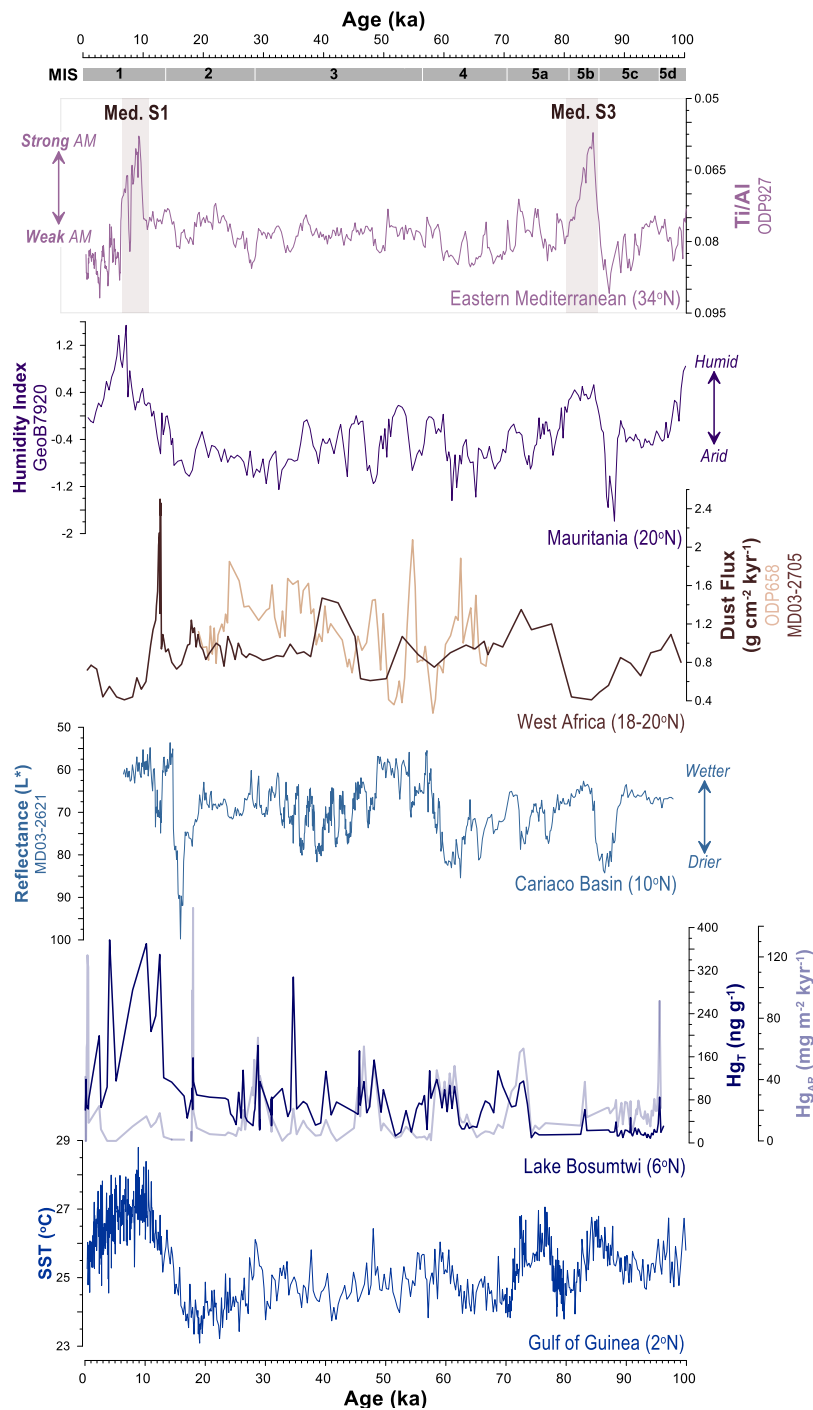
Figure 5: Records of total mercury (Hg$_T$) and mercury accumulation rate (Hg$_{AR}$) for Lake Bosumtwi generated by this study, compared with key paleoclimate records presented in order of latitude (physical locations shown in **Figure 1**). Sea-surface temperature (SST) reconstructed in core MD03-2707 from the Gulf of Guinea (Weldeab et al., 2007). Sediment total reflectance (L*) in marine core MD03-2621 from offshore South America (Cariaco Basin, Venezuela) as a proxy for oscillations in mean ITCZ position, and hydrological conditions anticipated in light of these oscillations over West Africa (Deplazes et al., 2013). Dust fluxes recorded in cores ODP658 (Cap Blanc; Kinsley et al., 2022) and MD03-2705 (; Skonieczny et al., 2019), and a continental humidity index of core GeoB7920-2 (Mauritanian seamount; Tjallingii et al., 2008) – all from offshore Mauritania. Finally, Ti/Al recorded in core ODP 927 from the Eastern Mediterranean as a record of riverine (low Ti/Al) versus aeolian (high Ti/Al) North African inputs to the Mediterranean basin, with low values reflecting a more intense African monsoon (Grant et al., 2022, 2017). Mediterranean sapropels one (Med. S1) and three (Med. S3) are marked by light brown bars (Grant et al., 2016). Light grey bars mark marine isotope stages (MIS) defined by the LR04 benthic marine isotope stack (Lisiecki and Raymo, 2005).

Hydroclimate was a key driver of changes in fire activity in tropical sub-Saharan Africa during the late Pleistocene (Moore et al. 2022). However, although wetter climatic conditions may be broadly associated with heightened fire activity due to associated increases in terrestrial biomass, recent work has shown that discrete changes in precipitation can elicit notably different fire responses between sites (e.g., Gosling et al., 2021; Karp et al., 2023). The influence of biomass burning on the Hg record presented here appears similarly complex; despite being a well-constrained factor in the Bosumtwi catchment, and evidence that wildfires are also a significant source of Hg, accounting for ~13% of natural Hg (re-)emissions to the modern atmosphere (Francisco López et al., 2022). Given that no clear relation is visible between Hg$_T$, Hg$_{AR}$, and two discrete macro- (Kiely, 2023) and micro- (Miller et al., 2016) charcoal profiles generated from the BOS04-5B core, we suggest that the effects of Hg emitted during wildfires did not leave a clear imprint on Hg variability in this record (**Fig. S8**).

Hydroclimate was a dominant driver of changes in fire activity in sub-Saharan Africa during the late Pleistocene. Wetter climatic conditions are typically associated with heightened fire activity due to associated increases in terrestrial biomass (e.g., Gosling et al., 2021; Moore et al., 2022), and wildfires are also a significant source of Hg, accounting for ~13% of natural Hg (re-)emissions to the modern atmosphere (Francisco López et al., 2022). The influence of biomass burning on the Hg record presented here is less clear; despite being a well-constrained factor in the Bosumtwi catchment. No clear correlation is visible between Hg$_T$, Hg$_{AR}$, and two discrete macro- (Kiely, 2023) and micro- (Miller et al., 2016) charcoal profiles generated from the BOS04-5B core, suggesting that the effects of Hg emitted during wildfires did not leave a clear imprint on Hg variability in this record (**Fig. S8**).

6. Synthesis and conclusions

This study combines new sedimentary Hg data from Lake Bosumtwi, Ghana, with proxy data from archives across the African continent to explore whether hydroclimate has exerted a measurable

651 effect on regional Hg cycling over the past ~96-kyr. ~~This study seeks a better understanding of the~~
652 ~~impact that local, climate-driven environmental shifts may have on the terrestrial Hg cycle over~~
653 ~~multiple millennia~~. The resolution of the BOS04-5B record (~0.6 k~~yr~~a per sample) precludes a detailed
654 assessment of more recent (<0.2-kyr), anthropogenic-driven changes in local Hg cycling. However,
655 this record is well suited for a broader exploration of patterns and drivers of variability in sedimentary
656 Hg concentrations in Lake Bosumtwi during the late Pleistocene. Combining our results with existing
657 data reveals two possible drivers of variability in Hg_T and Hg_{AR} in Lake Bosumtwi on these timescales:
658 organic matter (host) availability, and local-scale changes in Hg input to the lake by precipitation (**Fig.**
659 **4**). Both are intrinsically coupled to the local hydroclimate by their link to the lake level, with higher
660 lake levels typically corresponding to wetter conditions in the catchment, and deposition of more
661 organic-rich sediments. **Figure 6** illustrates how selected environmental processes, under different
662 environmental conditions, may have interacted with these two drivers to control Hg burial in Lake
663 Bosumtwi between ~96 and 0 ka. Considered together, the evidence summarised in panels **(1), (2),**
664 and **(2a)** all suggest that rates of Hg drawdown in Lake Bosumtwi, and indeed the signals retained in
665 the sediment record, reflect changes in net Hg supply from the atmosphere.

666 Between ~96 and 73 ka (**Fig. 6, panel (1)**), generally arid conditions shifted the lake into a negative
667 water balance. Not only could this have reduced the net flux of Hg to the lake by wet deposition
668 (precipitation), but a negative water balance would also limit internal primary productivity and
669 preservation, and so render less organic material available to sequester any Hg present in the
670 system. Secondary dilution of Hg by detrital materials could have also lowered sedimentary Hg
671 concentrations, with elevated sediment delivery to the BOS04 site driven by exposure of the steep-
672 sided crater walls during lake level lowering, and heightened soil instability due to widespread
673 recession of catchment vegetation. All would persist (if not strengthen) during AI-1, and so could
674 explain the lack of any measurable changes in Hg_T and Hg_{AR} during this time.

675 Following an extended period of aridity, net supply of Hg to the basin would be increased by
676 precipitation following ~73 ka, which would simultaneously cause the lake to become deeper and
677 more stratified (**Fig. 6, panel (2)**). As the bottom waters became more oxygen-depleted, more
678 effective organic matter burial would simultaneously enhance Hg drawdown compared to detrital
679 mineral supply; with higher lake levels, vegetation growth, and soil stabilization preventing exposure
680 and erosion of the crater walls and soils surrounding the lake. Hence, this abrupt shift to humid (net-
681 positive precipitation-evaporation balance) conditions in the Bosumtwi catchment could plausibly have
682 driven an increase in sedimentary Hg concentrations and accumulation, by eliciting a pronounced rise
683 in lake level as well as increasing the atmospheric Hg flux.

684 The processes described in panel (2) would be amplified further between ~15 and 4 ka (**Fig. 6, panel**
685 **2a**). Corresponding to Bosumtwi sapropel unit 1, this unit marks a distinct humid period characterised
686 by anomalously high rainfall, and documented by proxy records across sub-Saharan Africa
687 (Shanahan et al., 2015). For a closed lake system such as Lake Bosumtwi, these wetter conditions
688 would drive a sharp increase in lake depth, stratification, and scavenging in the water column – all of
689 which could favour heightened Hg drawdown to the sediment. 'Flattening' of the Hg-TOC relationship

690 during this interval also suggests that the Hg supply was (far) exceeded by the organic matter
691 availability (**Fig. S3a**), and so elevated Hg supply by precipitation could explain why Hg_T and Hg_{AR}
692 values are so unusually high (**Fig. 4a, 5**).
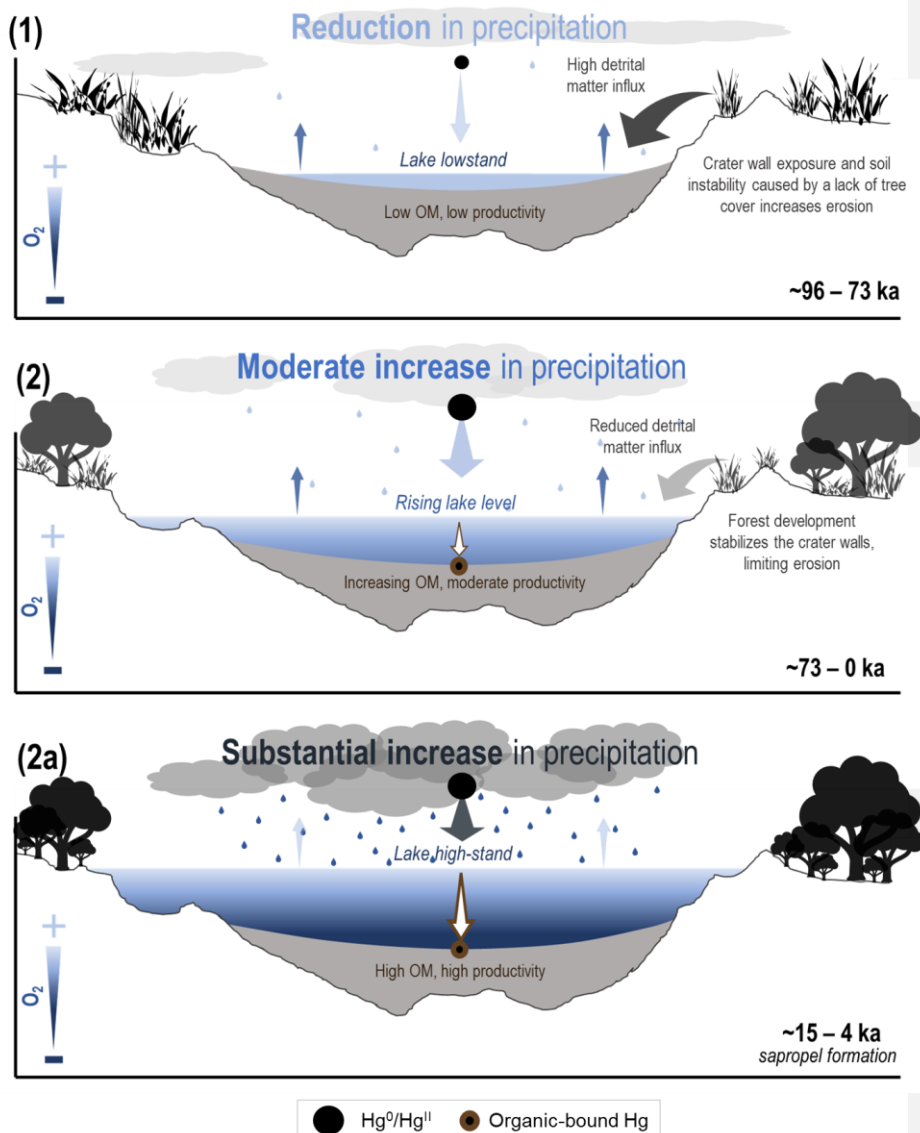
Figure 6: Schematic model depicting the processes that may control Hg flux, accumulation, and burial in Lake Bosumtwi under **(1)** arid (~93 – 73 ka), and **(2)** humid (~73 – 0 ka), environmental conditions. Panel **(2a)** depicts the very humid conditions that would be conducive to sapropel formation, such as those known to have occurred during the African Humid Period (~15 – 4 ka). Taken together, Hg fluxes increase during wet periods due to higher wet deposition directly to the lake relative to evasion, and/or by enhanced mobilization and transport of Hg from the catchment. Hg sequestration can also be enhanced by OM-scavenging in the water column, and increased lake stratification (anoxia at lake floor). The opposite occurs during dry intervals.

693   Future research should seek better constraints on how basin-specific variations in sediment

694   composition, lake structure, and water balance may influence how sedimentary Hg signals are

695   preserved and interpreted. This is because all could produce diverse, and perhaps contrasting, results

696   between lake systems. For example, results from Lake Bosumtwi suggest that lakes with smaller

697   watersheds, simple morphology, and minimal hydrological connectivity to the catchment could be

698   suitable targets to study catchment and intra-lake depositional processes over multiple millennia.

699   However, there are currently too few records covering these timescales to say this with certainty, and

700   not all closed lakes record measurable changes in Hg composition corresponding to changes in local

701   hydroclimate (Lent and Alexander, 1996; Pompeani et al., 2018). Organic matter/host phase

702   availability also appears to represent just one of several possible processes governing Hg burial in

703   lacustrine systems, given these systems are more readily affected by short-term changes in erosion,

704   nutrients, water balance, and catchment hydrology (Paine et al., 2024; Schütze et al., 2021).

705   Lake Bosumtwi is a small, morphologically simple lake. However, the complexity shown by its

706   sedimentary Hg record suggests that identical stratigraphic signals are unlikely to be recorded in

707   separate lakes, even if they are dominated by one common process, mechanism, and/or structure.

708   Exploring the importance of hydroclimate for Hg cycling relative to different catchment to lake area

709   ratios, hydrology (e.g., endorheic (closed) versus exoreic (open)), and/or catchment structures (e.g.,

710   forest versus savannah) would undoubtedly help to better resolve processes acting on single

711   lacustrine and terrestrial successions, but also identify the systems that may more sensitively record

712   major changes in Hg cycling. Provided the hydrological component of the Hg cycle can be isolated,

713   better characterization of the processes impacting lacustrine Hg cycling could also allow this element

714   to be used as a proxy for hydroclimatic change in terrestrial archives. For example, measurement of

715   sedimentary Hg isotopes in low-latitude and/or closed lakes could help quantify the contribution of Hg

716   to the sediment from precipitation or dry deposition, shedding new light on key biogeochemical

717   reaction pathways, processes (e.g., mass-independent fractionation (MIF)), and responses to

718   changing local hydrology across a range of timescales (e.g., Blum et al., 2014; Gao et al., 2023; Yin

719   et al., 2024).

720

721   This study provides new and valuable evidence for long-term interactions between terrestrial Hg

722   cycling and hydroclimate, and demonstrates that hydroclimate may be a key driver of Hg cycling in

723   tropical lakes over millennial-timescales. The sparse number of continuous, pre-industrial Hg records

724   currently available for sub-Saharan Africa have historically limited the ability to understand the extent

725   to which hydroclimate may drive long-term (>10^2-year) variability in the Hg cycle (Schneider et al.,

726   2023), and subsequently how this relationship is represented in local and global ecosystem models

727 (Cooke et al., 2020; Obrist et al., 2018). Although this knowledge gap cannot be satisfied by a single

728 record, study of Lake Bosumtwi reinforces the value of these records for better characterization of the

729 Hg behaviour likely to be associated with projected future, monsoon-driven, hydroclimate variability

730 (Chang et al., 2022). In time, this could translate to better understanding of how the tropical Hg cycle

731 may respond to future, global-scale changes (Gustin et al., 2020; Schneider et al., 2023).

732

Competing Interests

734 The contact author has declared that none of the authors has any competing interests.

Acknowledgements

736 ARP, IMF, JF, and TAM acknowledge funding from European Research Council Consolidator Grant

737 V-ECHO (ERC-2018-COG-8187 17-V-ECHO). ARP thanks Christopher Scholz for provision of

738 sediment data, alongside James Bryson, Alex Dickson, and Erdem Idiz for insightful discussions in

739 early stages of manuscript preparation. Thanks also go to Stephen Wyatt (University of Oxford) for

740 analytical assistance throughout the study. All authors thank members of the International Continental

741 Scientific Drilling Program Lake Bosumtwi Drilling Project: for their efforts in extracting and producing

742 the sediment succession, and making the data available for scientific use.

743

References

745 Åkerblom, S., Bishop, K., Björn, E., Lambertsson, L., Eriksson, T., Nilsson, M.B., 2013. Significant interaction
746   effects from sulfate deposition and climate on sulfur concentrations constitute major controls on
747   methylmercury production in peatlands. Geochimica et Cosmochimica Acta 102, 1–11.
748   https://doi.org/10.1016/j.gca.2012.10.025
749 Amos, H.M., Sonke, J.E., Obrist, D., Robins, N., Hagan, N., Horowitz, H.M., Mason, R.P., Witt, M., Hedgecock,
750   I.M., Corbitt, E.S., Sunderland, E.M., 2015. Observational and modeling constraints on global
751   anthropogenic enrichment of mercury. Environmental Science and Technology 49, 4036–4047.
752   https://doi.org/10.1021/es5058665
753 Armenteros, I., 2010. Diagenesis of Carbonates in Continental Settings, in: Developments in Sedimentology.
754   Elsevier, pp. 61–151. https://doi.org/10.1016/S0070-4571(09)06202-5
755 Armstrong, E., Tallavaara, M., Hopcroft, P.O., Valdes, P.J., 2023. North African humid periods over the past
756   800,000 years. Nat Commun 14, 5549. https://doi.org/10.1038/s41467-023-41219-4
757 Baxter, A.J., Verschuren, D., Peterse, F., Miralles, D.G., Martin-Jones, C.M., Maitituerdi, A., Van Der Meeren, T.,
758   Van Daele, M., Lane, C.S., Haug, G.H., Olago, D.O., Sinninghe Damsté, J.S., 2023. Reversed Holocene
759   temperature–moisture relationship in the Horn of Africa. Nature 620, 336–343.
760   https://doi.org/10.1038/s41586-023-06272-5
761 Benoit, J.M., Gilmour, C.C., Mason, R.P., Heyes, A., 1999. Sulfide controls on mercury speciation and
762   bioavailability to methylating bacteria in sediment pore waterA. Environmental Science and Technology
763   33, 1780. https://doi.org/10.1021/es992007q
764 Bertrand, S., Tjallingii, R., Kylander, M.E., Wilhelm, B., Roberts, S.J., Arnaud, F., Brown, E., Bindler, R., 2024.
765   Inorganic geochemistry of lake sediments: A review of analytical techniques and guidelines for data
766   interpretation. Earth-Science Reviews 249, 104639. https://doi.org/10.1016/j.earscirev.2023.104639
767 Biester, H., Pérez-Rodríguez, M., Gilfedder, B.-S., Martínez Cortizas, A., Hermanns, Y.-M., 2018. Solar
768   irradiance and primary productivity controlled mercury accumulation in sediments of a remote lake in the
769   Southern Hemisphere during the past 4000 years: Primary productivity and mercury accumulation.
770   Limnol. Oceanogr. 63, 540–549. https://doi.org/10.1002/lno.10647
771 Bin, C., Xiaoru, W., Lee, F.S.C., 2001. Pyrolysis coupled with atomic absorption spectrometry for the
772   determination of mercury in Chinese medicinal materials. Analytica Chimica Acta 447, 161–169.
773   https://doi.org/10.1016/S0003-2670(01)01218-1
774 Bishop, K., Shanley, J.B., Riscassi, A., de Wit, H.A., Eklöf, K., Meng, B., Mitchell, C., Osterwalder, S., Schuster,
775   P.F., Webster, J., Zhu, W., 2020. Recent advances in understanding and measurement of mercury in

the environment: Terrestrial Hg cycling. Science of the Total Environment 721. https://doi.org/10.1016/j.scitotenv.2020.137647

Blais, J.M., Kalff, J., 1995. The influence of lake morphometry on sediment focusing. Limnol. Oceanogr. 40, 582–588. https://doi.org/10.4319/lo.1995.40.3.0582

Blum, J.D., Sherman, L.S., Johnson, M.W., 2014. Mercury Isotopes in Earth and Environmental Sciences. Annu. Rev. Earth Planet. Sci. 42, 249–269. https://doi.org/10.1146/annurev-earth-050212-124107

Boamah, D., Koeberl, C., 2007. The Lake Bosumtwi impact structure in Ghana: A brief environmental assessment and discussion of ecotourism potential. Meteoritics and Planetary Science 42, 561–567. https://doi.org/10.1111/j.1945-5100.2007.tb01061.x

Bradley, R.S., Diaz, H.F., 2021. Late Quaternary Abrupt Climate Change in the Tropics and Sub-Tropics: The Continental Signal of Tropical Hydroclimatic Events (THEs). Reviews of Geophysics 59, e2020RG000732. https://doi.org/10.1029/2020RG000732

Branfireun, B.A., Cosio, C., Poulain, A.J., Riise, G., Bravo, A.G., 2020. Mercury cycling in freshwater systems - An updated conceptual model. Science of the Total Environment 745. https://doi.org/10.1016/j.scitotenv.2020.140906

Bravo, A.G., Bouchet, S., Tolu, J., Björn, E., Mateos-Rivera, A., Bertilsson, S., 2017. Molecular composition of organic matter controls methylmercury formation in boreal lakes. Nat Commun 8, 14255. https://doi.org/10.1038/ncomms14255

Brodie, C.R., Leng, M.J., Casford, J.S.L., Kendrick, C.P., Lloyd, J.M., Yongqiang, Z., Bird, M.I., 2011. Evidence for bias in C and N concentrations and δ13C composition of terrestrial and aquatic organic materials due to pre-analysis acid preparation methods. Chemical Geology 282, 67–83. https://doi.org/10.1016/j.chemgeo.2011.01.007

Brooks, K., Scholz, C.A., King, J.W., Peck, J., Overpeck, J.T., Russell, J.M., Amoako, P.Y.O., 2005. Late-Quaternary lowstands of lake Bosumtwi, Ghana: Evidence from high-resolution seismic-reflection and sediment-core data. Palaeogeography, Palaeoclimatology, Palaeoecology 216, 235–249. https://doi.org/10.1016/j.palaeo.2004.10.005

Brumsack, H.J., 2006. The trace metal content of recent organic carbon-rich sediments: Implications for Cretaceous black shale formation. Palaeogeography, Palaeoclimatology, Palaeoecology 232, 344–361. https://doi.org/10.1016/j.palaeo.2005.05.011

Chang, M., Liu, B., Wang, B., Martinez-Villalobos, C., Ren, G., Zhou, T., 2022. Understanding Future Increases in Precipitation Extremes in Global Land Monsoon Regions. Journal of Climate 35, 1839–1851. https://doi.org/10.1175/JCLI-D-21-0409.1

Chede, B.S., Venancio, I.M., Figueiredo, T.S., Albuquerque, A.L.S., Silva-Filho, E.V., 2022. Mercury deposition in the western tropical South Atlantic during the last 70 ka. Palaeogeography, Palaeoclimatology, Palaeoecology 601, 111122. https://doi.org/10.1016/j.palaeo.2022.111122

Cohen, A., Campisano, C., Arrowsmith, R., Asrat, A., Behrensmeyer, A.K., Deino, A., Feibel, C., Hill, A., Johnson, R., Kingston, J., Lamb, H., Lowenstein, T., Noren, A., Olago, D., Owen, R.B., Potts, R., Reed, K., Renaut, R., Schäbitz, F., Tiercelin, J.-J., Trauth, M.H., Wynn, J., Ivory, S., Brady, K., O'Grady, R., Rodysill, J., Githiri, J., Russell, J., Foerster, V., Dommain, R., Rucina, S., Deocampo, D., Russell, J., Billingsley, A., Beck, C., Dorenbeck, G., Dullo, L., Feary, D., Garello, D., Gromig, R., Johnson, T., Junginger, A., Karanja, M., Kimburi, E., Mbuthia, A., McCartney, T., McNulty, E., Muiruri, V., Nambiro, E., Negash, E.W., Njagi, D., Wilson, J.N., Rabideaux, N., Raub, T., Sier, M.J., Smith, P., Urban, J., Warren, M., Yadeta, M., Yost, C., Zinaye, B., 2016. The Hominin Sites and Paleolakes Drilling Project: inferring the environmental context of human evolution from eastern African rift lake deposits. Sci. Dril. 21, 1–16. https://doi.org/10.5194/sd-21-1-2016

Cohen, A.S., Campisano, C.J., Arrowsmith, J.R., Asrat, A., Beck, C.C., Behrensmeyer, A.K., Deino, A.L., Feibel, C.S., Foerster, V., Kingston, J.D., Lamb, H.F., Lowenstein, T.K., Lupien, R.L., Muiruri, V., Olago, D.O., Owen, R.B., Potts, R., Russell, J.M., Schaebitz, F., Stone, J.R., Trauth, M.H., Yost, C.L., 2022. Reconstructing the Environmental Context of Human Origins in Eastern Africa Through Scientific Drilling. Annu. Rev. Earth Planet. Sci. 50, 451–476. https://doi.org/10.1146/annurev-earth-031920-081947

Cohen, A.S., Stone, J.R., Beuning, K.R.M., Park, L.E., Reinthal, P.N., Dettman, D., Scholz, C.A., Johnson, T.C., King, J.W., Talbot, M.R., Brown, E.T., Ivory, S.J., 2007. Ecological consequences of early Late Pleistocene megadroughts in tropical Africa. Proc. Natl. Acad. Sci. U.S.A. 104, 16422–16427. https://doi.org/10.1073/pnas.0703873104

Cooke, C.A., Martínez-Cortizas, A., Bindler, R., Sexauer Gustin, M., 2020. Environmental archives of atmospheric Hg deposition – A review. Science of the Total Environment 709, 134800. https://doi.org/10.1016/j.scitotenv.2019.134800

Crocker, A.J., Naafs, B.D.A., Westerhold, T., James, R.H., Cooper, M.J., Röhl, U., Pancost, R.D., Xuan, C., Osborne, C.P., Beerling, D.J., Wilson, P.A., 2022. Astronomically controlled aridity in the Sahara since at least 11 million years ago. Nat. Geosci. 15, 671–676. https://doi.org/10.1038/s41561-022-00990-7

deMenocal, P.B., 1995. Plio-Pleistocene African Climate. Science 270, 53–59. https://doi.org/10.1126/science.270.5233.53

Deplazes, G., Lückge, A., Peterson, L.C., Timmermann, A., Hamann, Y., Hughen, K.A., Röhl, U., Laj, C., Cane, M.A., Sigman, D.M., Haug, G.H., 2013. Links between tropical rainfall and North Atlantic climate during the last glacial period. Nature Geoscience 6, 213–217. https://doi.org/10.1038/ngeo1712

Edwards, B.A., Kushner, D.S., Outridge, P.M., Wang, F., 2021. Fifty years of volcanic mercury emission research: Knowledge gaps and future directions. Science of the Total Environment 757, 143800. https://doi.org/10.1016/j.scitotenv.2020.143800

Engstrom, D.R., Rose, N.L., 2013. A whole-basin, mass-balance approach to paleolimnology. J Paleolimnol 49, 333–347. https://doi.org/10.1007/s10933-012-9675-5

Fadina, O.A., Venancio, I.M., Belem, A., Silveira, C.S., Bertagnolli, D. de C., Silva-Filho, E.V., Albuquerque, A.L.S., 2019. Paleoclimatic controls on mercury deposition in northeast Brazil since the Last Interglacial. Quaternary Science Reviews 221, 105869. https://doi.org/10.1016/j.quascirev.2019.105869

Figueiredo, T.S., Bergquist, B.A., Santos, T.P., Albuquerque, A.L.S., Silva-Filho, E.V., 2022. Relationship between glacial CO2 drawdown and mercury cycling in the western South Atlantic: An isotopic insight. Geology 50, 3–7. https://doi.org/10.1130/g49942.1

Foerster, V., Asrat, A., Bronk Ramsey, C., Brown, E.T., Chapot, M.S., Deino, A., Duesing, W., Grove, M., Hahn, A., Junginger, A., Kaboth-Bahr, S., Lane, C.S., Opitz, S., Noren, A., Roberts, H.M., Stockhecke, M., Tiedemann, R., Vidal, C.M., Vogelsang, R., Cohen, A.S., Lamb, H.F., Schaebitz, F., Trauth, M.H., 2022. Pleistocene climate variability in eastern Africa influenced hominin evolution. Nat. Geosci. 15, 805–811. https://doi.org/10.1038/s41561-022-01032-y

Francisco López, A., Heckenauer Barrón, E.G., Bello Bugallo, P.M., 2022. Contribution to understanding the influence of fires on the mercury cycle: Systematic review, dynamic modelling and application to sustainable hypothetical scenarios. Environ Monit Assess 194, 707. https://doi.org/10.1007/s10661-022-10208-3

Frieling, J., Mather, T.A., März, C., Jenkyns, H.C., Hennekam, R., Reichart, G.-J., Slomp, C.P., Van Helmond, N.A.G.M., 2023. Effects of redox variability and early diagenesis on marine sedimentary Hg records. Geochimica et Cosmochimica Acta S0016703723001850. https://doi.org/10.1016/j.gca.2023.04.015

Gao, X., Yuan, W., Chen, J., Huang, F., Wang, Z., Gong, Y., Zhang, Y., Liu, Y., Zhang, T., Zheng, W., 2023. Tracing the source and transport of Hg during pedogenesis in strongly weathered tropical soil using Hg isotopes. Geochimica et Cosmochimica Acta 361, 101–112. https://doi.org/10.1016/j.gca.2023.10.009

Gehrke, G.E., Blum, J.D., Meyers, P.A., 2009. The geochemical behavior and isotopic composition of Hg in a mid-Pleistocene western Mediterranean sapropel. Geochimica et Cosmochimica Acta 73, 1651–1665. https://doi.org/10.1016/j.gca.2008.12.012

Gosling, W.D., McMichael, C.N.H., Groenwoud, Z., Roding, E., Miller, C.S., Julier, A.C.M., 2021. Preliminary evidence for green, brown and black worlds in tropical western Africa during the Middle and Late Pleistocene. Palaeoecology of Africa 35, 13–25. https://doi.org/10.1201/9781003162766

Gosling, W.D., Miller, C.S., Shanahan, T.M., Holden, P.B., Overpeck, J.T., van Langevelde, Frank., 2022a. A stronger role for long-term moisture change than for CO2 in determining tropical woody vegetation change. Science 376, 653–656. https://doi.org/10.1126/science.abg4618

Gosling, W.D., Scerri, E.M.L., Kaboth-Bahr, S., 2022b. The climate and vegetation backdrop to hominin evolution in Africa. Philosophical Transactions of the Royal Society B: Biological Sciences 377. https://doi.org/10.1098/rstb.2020.0483

Grant, K.M., Amarathunga, U., Amies, J.D., Hu, P., Qian, Y., Penny, T., Rodriguez-Sanz, L., Zhao, X., Heslop, D., Liebrand, D., Hennekam, R., Westerhold, T., Gilmore, S., Lourens, L.J., Roberts, A.P., Rohling, E.J., 2022. Organic carbon burial in Mediterranean sapropels intensified during Green Sahara Periods since 3.2 Myr ago. Commun Earth Environ 3, 11. https://doi.org/10.1038/s43247-021-00339-9

Grant, K.M., Grimm, R., Mikolajewicz, U., Marino, G., Ziegler, M., Rohling, E.J., 2016. The timing of Mediterranean sapropel deposition relative to insolation, sea-level and African monsoon changes. Quaternary Science Reviews 140, 125–141. https://doi.org/10.1016/j.quascirev.2016.03.026

Grant, K.M., Rohling, E.J., Westerhold, T., Zabel, M., Heslop, D., Konijnendijk, T., Lourens, L., 2017. A 3 million year index for North African humidity/aridity and the implication of potential pan-African Humid periods. Quaternary Science Reviews 171, 100–118. https://doi.org/10.1016/j.quascirev.2017.07.005

Grygar, T.M., Mach, K., Martinez, M., 2019. Checklist for the use of potassium concentrations in siliciclastic sediments as paleoenvironmental archives. Sedimentary Geology 382, 75–84. https://doi.org/10.1016/j.sedgeo.2019.01.010

Guédron, S., Ledru, M.P., Escobar-Torrez, K., Develle, A.L., Brisset, E., 2018. Enhanced mercury deposition by Amazonian orographic precipitation: Evidence from high-elevation Holocene records of the Lake Titicaca region (Bolivia). Palaeogeography, Palaeoclimatology, Palaeoecology 511, 577–587. https://doi.org/10.1016/j.palaeo.2018.09.023

Gulati, R.D., Zadereev, E.S., Degermendzhi, A.G. (Eds.), 2017. Ecology of Meromictic Lakes, Ecological Studies. Springer International Publishing, Cham. https://doi.org/10.1007/978-3-319-49143-1

Gustin, M.S., Bank, M.S., Bishop, K., Bowman, K., Branfireun, B., Chételat, J., Eckley, C.S., Hammerschmidt, C.R., Lamborg, C., Lyman, S., Martínez-Cortizas, A., Sommar, J., Tsui, M.T.-K., Zhang, T., 2020. Mercury biogeochemical cycling: A synthesis of recent scientific advances. Science of The Total Environment 737, 139619. https://doi.org/10.1016/j.scitotenv.2020.139619

Ha, J., Zhao, X., Yu, R., Barkay, T., Yee, N., 2017. Hg(II) reduction by siderite ($FeCO_3$). Applied Geochemistry 78, 211-218. https://doi.org/10.1016/j.apgeochem.2016.12.017

Hammer, Ø., Harper, D.A.T., Ryan, P.D., 2001. PAST: Paleontological statistics software package for education and data analysis. Palaeontologia Electronica 4, 9.

907 Han, S., Obraztsova, A., Pretto, P., Deheyn, D.D., Gieskes, J., Tebo, B.M., 2008. Sulfide and iron control on
908   mercury speciation in anoxic estuarine sediment slurries. Marine Chemistry 111, 214–220.
909   https://doi.org/10.1016/j.marchem.2008.05.002
910 Hermanns, Y.M., Biester, H., 2013. A 17,300-year record of mercury accumulation in a pristine lake in southern
911   Chile. Journal of Paleolimnology 49, 547–561. https://doi.org/10.1007/s10933-012-9668-4
912 Hermanns, Y.M., Cortizas, A.M., Arz, H., Stein, R., Biester, H., 2013. Untangling the influence of in-lake
913   productivity and terrestrial organic matter flux on 4,250 years of mercury accumulation in Lake Hambre,
914   Southern Chile. Journal of Paleolimnology 49, 563–573. https://doi.org/10.1007/s10933-012-9657-7
915 Hernández, A., Martin-Puertas, C., Moffa-Sánchez, P., Moreno-Chamarro, E., Ortega, P., Blockley, S., Cobb, K.,
916   Comas-Bru, L., Giralt, S., Goosse, H., Luterbacher, J., Martrat, B., Muscheler, R., Parnell, A., Pla-
917   Rabes, S., Sjolte, J., Scaife, A., Swingedouw, D., Wise, E., Xu, G., 2020. Modes of climate variability:
918   Synthesis and review of proxy-based reconstructions through the Holocene. Earth-Science Reviews
919   209, 103286. https://doi.org/10.1016/j.earscirev.2020.103286
920 Hsu-Kim, H., Kucharzyk, K.H., Zhang, T., Deshusses, M.A., 2013. Mechanisms Regulating Mercury
921   Bioavailability for Methylating Microorganisms in the Aquatic Environment: A Critical Review. Environ.
922   Sci. Technol. 47, 2441–2456. https://doi.org/10.1021/es304370g
923 Jenkyns, H.C., 1988. The Early Toarcian (Jurassic) Anoxic Event. American Journal of Science.
924 Jenkyns, H.C., Weedon, G.P., 2013. Chemostratigraphy (CaCO3, TOC, δ13Corg) of Sinemurian (Lower
925   Jurassic) black shales from the Wessex Basin, Dorset and palaeoenvironmental implications. nos 46, 1–
926   21. https://doi.org/10.1127/0078-0421/2013/0029
927 Jeon, B., Scircle, A., Cizdziel, J.V., Chen, J., Black, O., Wallace, D.J., Zhou, Y., Lepak, R.F., Hurley, J.P., 2020.
928   Historical deposition of trace metals in a marine sapropel from Mangrove Lake, Bermuda with emphasis
929   on mercury, lead, and their isotopic composition. J Soils Sediments 20, 2266–2276.
930   https://doi.org/10.1007/s11368-020-02567-6
931 Jones, W.B., Bacon, M., Hastings, D.A., 1981. The Lake Bosumtwi impact crater, Ghana. Geological Society of
932   America Bulletin 92, 342–349. https://doi.org/10.1130/0016-7606(1981)92<342:TLBICG>2.0.CO;2
933 Jourdan, F., Renne, P.R., Reimold, W.U., 2009. An appraisal of the ages of terrestrial impact structures. Earth
934   and Planetary Science Letters 286, 1–13. https://doi.org/10.1016/j.epsl.2009.07.009
935 Kaboth-Bahr, S., Gosling, W.D., Vogelsang, R., Bahr, A., Scerri, E.M.L., 2021. Paleo-ENSO influence on African
936   environments and early modern humans. Proceedings of the National Academy of Science 118, 1–6.
937   https://doi.org/10.1073/pnas.2018277118
938 Karp, A.T., Uno, K.T., Berke, M.A., Russell, J.M., Scholz, C.A., Marlon, J.R., Faith, J.T., Staver, A.C., 2023.
939   Nonlinear rainfall effects on savanna fire activity across the African Humid Period. Quaternary Science
940   Reviews 304, 107994. https://doi.org/10.1016/j.quascirev.2023.107994
941 Kiely, R., 2023. A 50,000-year reconstruction of West African fire history (MSc Thesis). University of Amsterdam,
942   Amsterdam.
943 Kinsley, C.W., Bradtmiller, L.I., McGee, D., Galgay, M., Stuut, J.B., Tjallingii, R., Winckler, G., DeMenocal, P.B.,
944   2022. Orbital and Millennial-Scale Variability in Northwest African Dust Emissions Over the Past 67,000
945   years. Paleoceanography and Paleoclimatology 37, 1–22. https://doi.org/10.1029/2020PA004137
946 Koeberl, C., Milkereit, B., Overpeck, J.T., Scholz, C.A., Amoako, P.Y.O., Boamah, D., Danuor, S.K., Karp, T.,
947   Kueck, J., Hecky, R.E., King, J.W., Peack, J.A., 2007. An international and multidisciplinary drilling
948   project into a young complex impact structure: The 2004 ICDP Bosumtwi Crater Drilling Project - An
949   overview. Meteoritics and Planetary Science 42, 483–511. https://doi.org/10.1111/j.1945-
950   5100.2007.tb01057.x
951 Koeberl, C., Peck, J., King, J., Milkereit, B., Overpeck, J., Scholz, C., 2005. The ICDP lake Bosumtwi drilling
952   project: A first report. Scientific Drilling 1, 23–27. https://doi.org/10.2204/iodp.sd.1.04.2005
953 Kuechler, R.R., Schefuß, E., Beckmann, B., Dupont, L., Wefer, G., 2013. NW African hydrology and vegetation
954   during the Last Glacial cycle reflected in plant-wax-specific hydrogen and carbon isotopes. Quaternary
955   Science Reviews 82, 56–67. https://doi.org/10.1016/j.quascirev.2013.10.013
956 Kuss, J., Zülicke, C., Pohl, C., Schneider, B., 2011. Atlantic mercury emission determined from continuous
957   analysis of the elemental mercury sea-air concentration difference within transects between 50°N and
958   50°S. Global Biogeochem. Cycles 25. https://doi.org/10.1029/2010GB003998
959 Larrasoaña, J.C., Roberts, A.P., Rohling, E.J., 2013. Dynamics of Green Sahara Periods and Their Role in
960   Hominin Evolution. PLoS ONE 8. https://doi.org/10.1371/journal.pone.0076514
961 Laskar, J., Robutel, P., Joutel, F., Gastineau, M., Correia, A.C.M., Levrard, B., 2004. A long-term numerical
962   solution for the insolation quantities of the Earth. Astronomy and Astrophysics 428, 261–285.
963   https://doi.org/10.1051/0004-6361:20041335
964 Leiva González, J., Diaz-Robles, L.A., Cereceda-Balic, F., Pino-Cortés, E., Campos, V., 2022. Atmospheric
965   Modelling of Mercury in the Southern Hemisphere and Future Research Needs: A Review. Atmosphere
966   13, 1226. https://doi.org/10.3390/atmos13081226
967 Lent, R.M., Alexander, C.R., 1996. Mercury accumulation in Devils Lake, north Dakota - effects of environmental
968   variation in closed-basin lakes on mercury chronologies. Water, Air, & Soil Pollution 98, 275–296.
969 Lézine, A.-M., Izumi, K., Kageyama, M., Achoundong, G., 2019. A 90,000-year record of Afromontane forest
970   responses to climate change. Science 363, 177–181. https://doi.org/10.1126/science.aav6821
971 Li, F., Ma, C., Zhang, P., 2020. Mercury Deposition, Climate Change and Anthropogenic Activities: A Review.
972   Frontiers in Earth Science 8, 316. https://doi.org/10.3389/feart.2020.00316

973 Lisiecki, L.E., Raymo, M.E., 2005a. A Pliocene-Pleistocene stack of 57 globally distributed benthic δ 18O
974   records. Paleoceanography 20, 1–17. https://doi.org/10.1029/2004PA001071
975 Lisiecki, L.E., Raymo, M.E., 2005b. A Pliocene-Pleistocene stack of 57 globally distributed benthic δ 18O
976   records. Paleoceanography 20, 1–17. https://doi.org/10.1029/2004PA001071
977 Liu, M., Zhang, Q., Maavara, T., Liu, S., Wang, X., Raymond, P.A., 2021. Rivers as the largest source of mercury
978   to coastal oceans worldwide. Nature Geoscience 14, 672–677. https://doi.org/10.1038/s41561-021-
979   00793-2
980 Lupien, R., Uno, K., Rose, C., deRoberts, N., Hazan, C., De Menocal, P., Polissar, P., 2023. Low-frequency
981   orbital variations controlled climatic and environmental cycles, amplitudes, and trends in northeast Africa
982   during the Plio-Pleistocene. Commun Earth Environ 4, 360. https://doi.org/10.1038/s43247-023-01034-7
983 Lyman, S.N., Cheng, I., Gratz, L.E., Weiss-Penzias, P., Zhang, L., 2020. An updated review of atmospheric
984   mercury. Science of the Total Environment 707, 135575. https://doi.org/10.1016/j.scitotenv.2019.135575
985 Machado, W., Sanders, C.J., Santos, I.R., Sanders, L.M., Silva-Filho, E.V., Luiz-Silva, W., 2016. Mercury dilution
986   by autochthonous organic matter in a fertilized mangrove wetland. Environmental Pollution 213, 30–35.
987   https://doi.org/10.1016/j.envpol.2016.02.002
988 Mason, R.P., Laporte, J.M., Andres, S., 2000. Factors controlling the bioaccumulation of mercury,
989   methylmercury, arsenic, selenium, and cadmium by freshwater invertebrates and fish. Archives of
990   Environmental Contamination and Toxicology 38, 283–297. https://doi.org/10.1007/s002449910038
991 McKay, N.P., 2012. A multidisciplinary approach to late Quaternary paleoclimatology with an emphasis on sub-
992   saharan West Africa and the last interglacial period (PhD Thesis). University of Arizona, Arizona.
993 Menviel, L., Govin, A., Avenas, A., Meissner, K.J., Grant, K.M., Tzedakis, P.C., 2021. Drivers of the evolution and
994   amplitude of African Humid Periods. Commun Earth Environ 2, 237. https://doi.org/10.1038/s43247-021-
995   00309-1
996 Miller, C.S., Gosling, W.D., 2014. Quaternary forest associations in lowland tropical West Africa. Quaternary
997   Science Reviews 84, 7–25. https://doi.org/10.1016/j.quascirev.2013.10.027
998 Miller, C.S., Gosling, W.D., Kemp, D.B., Coe, A.L., Gilmour, I., 2016. Drivers of ecosystem and climate change in
999   tropical West Africa over the past ~540 000 years. Journal of Quaternary Science 31, 671–677.
1000   https://doi.org/10.1002/jqs.2893
1001 Nalbant, J., Schneider, L., Hamilton, R., Connor, S., Biester, H., Stuart-Williams, H., Bergal-Kuvikas, O.,
1002   Jacobsen, G., Stevenson, J., 2023. Fire, volcanism and climate change: the main factors controlling
1003   mercury (Hg) accumulation rates in Tropical Lake Lantoa, Sulawesi, Indonesia (~16,500–540 cal yr BP).
1004   Front. Environ. Chem. 4, 1241176. https://doi.org/10.3389/fenvc.2023.1241176
1005 Nicholson, S.E., 2013. The West African Sahel: A Review of Recent Studies on the Rainfall Regime and Its
1006   Interannual Variability. ISRN Meteorology 2013, 1–32. https://doi.org/10.1155/2013/453521
1007 Obrist, D., Kirk, J.L., Zhang, L., Sunderland, E.M., Jiskra, M., Selin, N.E., 2018. A review of global environmental
1008   mercury processes in response to human and natural perturbations: Changes of emissions, climate, and
1009   land use. Ambio 47, 116–140. https://doi.org/10.1007/s13280-017-1004-9
1010 O'Mara, N.A., Skonieczny, C., McGee, D., Winckler, G., Bory, A.J.-M., Bradtmiller, L.I., Malaizé, B., Polissar, P.J.,
1011   2022. Pleistocene drivers of Northwest African hydroclimate and vegetation. Nat Commun 13, 3552.
1012   https://doi.org/10.1038/s41467-022-31120-x
1013 Outridge, P.M., Stern, G.A., Hamilton, P.B., Sanei, H., 2019. Algal scavenging of mercury in preindustrial Arctic
1014   lakes. Limnol Oceanogr 64, 1558–1571. https://doi.org/10.1002/lno.11135
1015 Outridge, Sanei, H., Stern, Hamilton, Goodarzi, F., 2007. Evidence for Control of Mercury Accumulation Rates in
1016   Canadian High Arctic Lake Sediments by Variations of Aquatic Primary Productivity. Environ. Sci.
1017   Technol. 41, 5259–5265. https://doi.org/10.1021/es070408x
1018 Paine, A.R., Fendley, I.M., Frieling, J., Mather, T.A., Lacey, J.H., Wagner, B., Robinson, S.A., Pyle, D.M.,
1019   Francke, A., Them II, T.R., Panagiotopoulos, K., 2024. Mercury records covering the past 90 000 years
1020   from lakes Prespa and Ohrid, SE Europe. Biogeosciences 21, 531–556. https://doi.org/10.5194/bg-21-
1021   531-2024
1022 Pan, J., Zhong, W., Wei, Z., Ouyang, J., Shang, S., Ye, S., Chen, Y., Xue, J., Tang, X., 2020. A 15,400-year
1023   record of natural and anthropogenic input of mercury (Hg) in a sub-alpine lacustrine sediment
1024   succession from the western Nanling Mountains, South China. Environmental Science and Pollution
1025   Research 27, 20478–20489. https://doi.org/10.1007/s11356-020-08421-z
1026 Pausata, F.S.R., Gaetani, M., Messori, G., Berg, A., Maia de Souza, D., Sage, R.F., deMenocal, P.B., 2020. The
1027   Greening of the Sahara: Past Changes and Future Implications. One Earth 2, 235–250.
1028   https://doi.org/10.1016/j.oneear.2020.03.002
1029 Peck, J.A., Green, R.R., Shanahan, T., King, J.W., Overpeck, J.T., Scholz, C.A., 2004. A magnetic mineral
1030   record of Late Quaternary tropical climate variability from Lake Bosumtwi, Ghana. Palaeogeography,
1031   Palaeoclimatology, Palaeoecology 215, 37–57. https://doi.org/10.1016/j.palaeo.2004.08.003
1032 Pérez-Rodríguez, M., Margalef, O., Corella, J.P., Saiz-Lopez, A., Pla-Rabes, S., Giralt, S., Cortizas, A.M., 2018.
1033   The role of climate: 71 ka of atmospheric mercury deposition in the southern hemisphere recorded by
1034   Rano Aroi Mire, Easter Island (Chile). Geosciences (Switzerland) 8.
1035   https://doi.org/10.3390/geosciences8100374
1036 Pilla, R.M., Williamson, C.E., Adamovich, B.V., Adrian, R., Anneville, O., Chandra, S., Colom-Montero, W.,
1037   Devlin, S.P., Dix, M.A., Dokulil, M.T., Gaiser, E.E., Girdner, S.F., Hambright, K.D., Hamilton, D.P.,
1038   Havens, K., Hessen, D.O., Higgins, S.N., Huttula, T.H., Huuskonen, H., Isles, P.D.F., Joehnk, K.D.,
1039   Jones, I.D., Keller, W.B., Knoll, L.B., Korhonen, J., Kraemer, B.M., Leavitt, P.R., Lepori, F., Luger, M.S.,

Maberly, S.C., Melack, J.M., Melles, S.J., Müller-Navarra, D.C., Pierson, D.C., Pislegina, H.V., Plisnier, P.-D., Richardson, D.C., Rimmer, A., Rogora, M., Rusak, J.A., Sadro, S., Salmaso, N., Saros, J.E., Saulnier-Talbot, É., Schindler, D.E., Schmid, M., Shimaraeva, S.V., Silow, E.A., Sitoki, L.M., Sommaruga, R., Straile, D., Strock, K.E., Thiery, W., Timofeyev, M.A., Verburg, P., Vinebrooke, R.D., Weyhenmeyer, G.A., Zadereev, E., 2020. Deeper waters are changing less consistently than surface waters in a global analysis of 102 lakes. Sci Rep 10, 20514. https://doi.org/10.1038/s41598-020-76873-x

Pompeani, D.P., Cooke, C.A., Abbott, M.B., Drevnick, P.E., 2018. Climate, Fire, and Vegetation Mediate Mercury Delivery to Midlatitude Lakes over the Holocene. Environmental Science and Technology 52, 8157–8164. https://doi.org/10.1021/acs.est.8b01523

Ravichandran, M., 2004. Interactions between mercury and dissolved organic matter - A review. Chemosphere 55, 319–331. https://doi.org/10.1016/j.chemosphere.2003.11.011

Russell, J., Talbot, M.R., Haskell, B.J., 2003. Mid-holocene climate change in Lake Bosumtwi, Ghana. Quaternary Research 60, 133–141. https://doi.org/10.1016/S0033-5894(03)00065-6

Sanei, H., Grasby, S., Beauchamp, B., 2012. Latest Permian mercury anomalies. Geology 40, 63–66.

Schneider, L., Cooke, C.A., Stansell, N.D., Haberle, S.G., 2020. Effects of climate variability on mercury deposition during the Older Dryas and Younger Dryas in the Venezuelan Andes. Journal of Paleolimnology 63, 211–224. https://doi.org/10.1007/s10933-020-00111-7

Schneider, L., Fisher, J.A., Diéguez, M.C., Fostier, A.-H., Guimaraes, J.R.D., Leaner, J.J., Mason, R., 2023. A synthesis of mercury research in the Southern Hemisphere, part 1: Natural processes. Ambio 52, 897–917. https://doi.org/10.1007/s13280-023-01832-5

Scholz, C.A., Johnson, T.C., Cohen, A.S., King, J.W., Peck, J.A., Overpeck, J.T., Talbot, M.R., Brown, E.T., Kalindekafe, L., Amoako, P.Y.O., Lyons, R.P., Shanahan, T.M., Castañeda, I.S., Heil, C.W., Forman, S.L., McHargue, L.R., Beuning, K.R., Gomez, J., Pierson, J., 2007. East African megadroughts between 135 and 75 thousand years ago and bearing on early-modern human origins. Proceedings of the National Academy of Sciences of the United States of America 104, 16416–16421. https://doi.org/10.1073/pnas.0703874104

Schultze, M., Boehrer, B., Wendt-Potthoff, K., Katsev, S., Brown, E.T., 2017. Chemical Setting and Biogeochemical Reactions in Meromictic Lakes, in: Ecology of Meromictic Lakes. Springer, pp. 35–61.

Schütze, M., Gatz, P., Gilfedder, B., Biester, H., 2021. Why productive lakes are larger mercury sedimentary sinks than oligotrophic brown water lakes. Limnol Oceanogr 66, 1316–1332. https://doi.org/10.1002/lno.11684

Schütze, M., Tserendorj, G., Pérez-Rodríguez, M., Rösch, M., Biester, H., 2018. Prediction of Holocene mercury accumulation trends by combining palynological and geochemical records of lake sediments (Black Forest, Germany). Geosciences (Switzerland) 8. https://doi.org/10.3390/geosciences8100358

Sebag, D., Garcin, Y., Adatte, T., Deschamps, P., Ménot, G., Verrecchia, E.P., 2018. Correction for the siderite effect on Rock-Eval parameters: Application to the sediments of Lake Barombi (southwest Cameroon). Organic Geochemistry 123, 126–135. https://doi.org/10.1016/j.orggeochem.2018.05.010

Segato, D., Saiz-Lopez, A., Mahajan, A.S., Wang, F., Corella, J.P., Cuevas, C.A., Erhardt, T., Jensen, C.M., Zeppenfeld, C., Kjær, H.A., Turetta, C., Cairns, W.R.L., Barbante, C., Spolaor, A., 2023. Arctic mercury flux increased through the Last Glacial Termination with a warming climate. Nat. Geosci. 16, 439–445. https://doi.org/10.1038/s41561-023-01172-9

Selin, N.E., 2009. Global biogeochemical cycling of mercury: a review. Annual Review of Environmental Resources 34, 43–63.

Shanahan, T.M., Beck, J.W., Overpeck, J.T., McKay, N.P., Pigati, J.S., Peck, J.A., Scholz, C.A., Heil, C.W., King, J., 2012. Late Quaternary sedimentological and climate changes at Lake Bosumtwi Ghana: New constraints from laminae analysis and radiocarbon age modeling. Palaeogeography, Palaeoclimatology, Palaeoecology 361–362, 49–60. https://doi.org/10.1016/j.palaeo.2012.08.001

Shanahan, T.M., Mckay, N.P., Hughen, K.A., Overpeck, J.T., Otto-Bliesner, B., Heil, C.W., King, J., Scholz, C.A., Peck, J., 2015. The time-transgressive termination of the African humid period. Nature Geoscience 8, 140–144. https://doi.org/10.1038/ngeo2329

Shanahan, T.M., Overpeck, J.T., Anchukaitis, K.J., Beck, J.W., Cole, J.E., Dettman, D.L., Peck, J.A., Scholz, C.A., King, J.W., 2009. Atlantic forcing of persistent drought in West Africa. Science 324, 377–380. https://doi.org/10.1126/science.1166352

Shanahan, T.M., Overpeck, J.T., Beck, J.W., Wheeler, C.W., Peck, J.A., King, J.W., Scholz, C.A., 2008a. The formation of biogeochemical laminations in Lake Bosumtwi, Ghana, and their usefulness as indicators of past environmental changes. Journal of Paleolimnology 40, 339–355. https://doi.org/10.1007/s10933-007-9164-4

Shanahan, T.M., Overpeck, J.T., Scholz, C.A., Beck, J.W., Peck, J., King, J.W., 2008b. Abrupt changes in the water balance of tropical West Africa during the late Quaternary. J. Geophys. Res. 113, D12108. https://doi.org/10.1029/2007JD009320

Shanahan, T.M., Overpeck, J.T., Sharp, W.E., Scholz, C.A., Arko, J.A., 2007. Simulating the response of a closed-basin lake to recent climate changes in tropical West Africa (Lake Bosumtwi, Ghana). Hydrological Processes 21, 1678–1691. https://doi.org/10.1002/hyp.6359

Shanahan, T.M., Overpeck, J.T., Wheeler, C.W., Beck, J.W., Pigati, J.S., Talbot, M.R., Scholz, C.A., Peck, J., King, J.W., 2006. Paleoclimatic variations in West Africa from a record of late Pleistocene and Holocene lake level stands of Lake Bosumtwi, Ghana. Palaeogeography, Palaeoclimatology, Palaeoecology 242, 287–302. https://doi.org/10.1016/j.palaeo.2006.06.007

Shanahan, T.M., Peck, J.A., McKay, N., Heil, C.W., King, J., Forman, S.L., Hoffmann, D.L., Richards, D.A., Overpeck, J.T., Scholz, C., 2013. Age models for long lacustrine sediment records using multiple dating approaches - An example from Lake Bosumtwi, Ghana. Quaternary Geochronology 15, 47–60. https://doi.org/10.1016/j.quageo.2012.12.001

Shen, J., Feng, Q., Algeo, T.J., Liu, Jinling, Zhou, C., Wei, W., Liu, Jiangsi, Them, T.R., Gill, B.C., Chen, J., 2020. Sedimentary host phases of mercury (Hg) and implications for use of Hg as a volcanic proxy. Earth and Planetary Science Letters 543, 116333. https://doi.org/10.1016/j.epsl.2020.116333

Skonieczny, C., McGee, D., Winckler, G., Bory, A., Bradtmiller, L.I., Kinsley, C.W., Polissar, P.J., De Pol-Holz, R., Rossignol, L., Malaizé, B., 2019. Monsoon-driven Saharan dust variability over the past 240,000 years. Science Advances 5, 1–9. https://doi.org/10.1126/sciadv.aav1887

Soerensen, A.L., Mason, R.P., Balcom, P.H., Jacob, D.J., Zhang, Y., Kuss, J., Sunderland, E.M., 2014. Elemental Mercury Concentrations and Fluxes in the Tropical Atmosphere and Ocean. Environ. Sci. Technol. 48, 11312–11319. https://doi.org/10.1021/es503109p

Sprovieri, F., Pirrone, N., Bencardino, M., D'Amore, F., Angot, H., Barbante, C., Brunke, E.-G., Arcega-Cabrera, F., Cairns, W., Comero, S., Diéguez, M. del C., Dommergue, A., Ebinghaus, R., Feng, X.B., Fu, X., Garcia, P.E., Gawlik, B.M., Hageström, U., Hansson, K., Horvat, M., Kotnik, J., Labuschagne, C., Magand, O., Martin, L., Mashyanov, N., Mkololo, T., Munthe, J., Obolkin, V., Ramirez Islas, M., Sena, F., Somerset, V., Spandow, P., Vardè, M., Walters, C., Wängberg, I., Weigelt, A., Yang, X., Zhang, H., 2017. Five-year records of mercury wet deposition flux at GMOS sites in the Northern and Southern hemispheres. Atmos. Chem. Phys. 17, 2689–2708. https://doi.org/10.5194/acp-17-2689-2017

Sprovieri, F., Pirrone, N., Ebinghaus, R., Kock, H., Dommergue, A., 2010. A review of worldwide atmospheric mercury measurements. Atmospheric Chemistry and Physics 10, 8245–8265. https://doi.org/10.5194/acp-10-8245-2010

Stager, J.C., Ryves, D.B., Chase, B.M., Pausata, F.S.R., 2011. Catastrophic Drought in the Afro-Asian Monsoon Region During Heinrich Event 1. Science 331, 1299–1302. https://doi.org/10.1126/science.1198322

Swart, P.K., 2015. The geochemistry of carbonate diagenesis: The past, present and future. Sedimentology 62, 1233–1304. https://doi.org/10.1111/sed.12205

Talbot, M.R., Johannessen, T., 1992. A high resolution palaeoclimatic record for the last 27,500 years in tropical West Africa from the carbon and nitrogen isotopic composition of lacustrine organic matter. Earth and Planetary Science Letters 110, 23–37. https://doi.org/10.1016/0012-821X(92)90036-U

Them, T.R., Jagoe, C.H., Caruthers, A.H., Gill, B.C., Grasby, S.E., Gröcke, D.R., Yin, R., Owens, J.D., 2019. Terrestrial sources as the primary delivery mechanism of mercury to the oceans across the Toarcian Oceanic Anoxic Event (Early Jurassic). Earth and Planetary Science Letters 507, 62–72. https://doi.org/10.1016/j.epsl.2018.11.029

Tisserand, D., Guédron, S., Viollier, E., Jézéquel, D., Rigaud, S., Campillo, S., Sarret, G., Charlet, L., Cossa, D., 2022. Mercury, organic matter, iron, and sulfur co-cycling in a ferruginous meromictic lake. Applied Geochemistry 146, 105463. https://doi.org/10.1016/j.apgeochem.2022.105463

Tjallingii, R., Claussen, M., Stuut, J.-B.W., Fohlmeister, J., Jahn, A., Bickert, T., Lamy, F., Röhl, U., 2008. Coherent high- and low-latitude control of the northwest African hydrological balance. Nature Geosci 1, 670–675. https://doi.org/10.1038/ngeo289

Trauth, M.H., Asrat, A., Berner, N., Bibi, F., Foerster, V., Grove, M., Kaboth-Bahr, S., Maslin, M.A., Mudelsee, M., Schäbitz, F., 2021. Northern Hemisphere Glaciation, African climate and human evolution. Quaternary Science Reviews 268, 107095. https://doi.org/10.1016/j.quascirev.2021.107095

Tribovillard, N., Algeo, T.J., Lyons, T., Riboulleau, A., 2006. Trace metals as paleoredox and paleoproductivity proxies: An update. Chemical Geology 232, 12–32. https://doi.org/10.1016/j.chemgeo.2006.02.012

Turner, B.F., Gardner, L.R., Sharp, W.E., 1996. The hydrology of lake Bosumtwi, a climate-sensitive lake in Ghana, West Africa. Journal of Hydrology 183, 243–261. https://doi.org/10.1016/0022-1694(95)02982-6

United Nations Environment Programme, 2018. Global Mercury Assessment, United Nations.

Vindušková, O., Jandová, K., Frouz, J., 2019. Improved method for removing siderite by *in situ* acidification before elemental and isotope analysis of soil organic carbon. J. Plant Nutr. Soil Sci. 182, 82–91. https://doi.org/10.1002/jpln.201800164

Vinnepand, M., Zeeden, C., Wonik, T., Gosling, W., Noren, A., Kück, J., Pierdominici, S., Voigt, S., Abadi, M.S., Ulfers, A., Danour, S., Afrifa, K., Kaboth-Bahr, S., 2024. An age-depth model for Lake Bosumtwi (Ghana) to reconstruct one million years of West African climate and environmental change. Quaternary Science Reviews 325, 108478. https://doi.org/10.1016/j.quascirev.2023.108478

Weldeab, S., Lea, D.W., Schneider, R.R., Andersen, N., 2007. 155,000 Years of West African Monsoon and Ocean Thermal Evolution. Science 316, 1303–1307. https://doi.org/10.1126/science.1140461

White, F. (Frank), 1983. The vegetation of Africa: a descriptive memoir to accompany the Unesco/AETFAT/UNSO vegetation map of Africa, Natural resources research ; 20. Unesco, Paris.

Woolway, R.I., Kraemer, B.M., Lenters, J.D., Merchant, C.J., O'Reilly, C.M., Sharma, S., 2020. Global lake responses to climate change. Nature Reviews Earth and Environment 1, 388–403. https://doi.org/10.1038/s43017-020-0067-5

Yin, R., Wang, X., Sun, R., Gao, L., Deng, C., Tian, Z., Luo, A., Lehmann, B., 2024. Linking the mercury biogeochemical cycle to the deep mercury cycle: A mercury isotope perspective. Chemical Geology 654, 122063. https://doi.org/10.1016/j.chemgeo.2024.122063

Zaferani, S., Biester, H., 2021. Mercury Accumulation in Marine Sediments – A Comparison of an Upwelling Area and Two Large River Mouths. Front. Mar. Sci. 8, 732720. https://doi.org/10.3389/fmars.2021.732720

Zolitschka, B., Francus, P., Ojala, A.E.K., Schimmelmann, A., 2015. Varves in lake sediments - a review. Quaternary Science Reviews 117, 1–41.

Zou, J., Chang, Y.P., Zhu, A., Chen, M.T., Kandasamy, S., Yang, H., Cui, J., Yu, P.S., Shi, X., 2021. Sedimentary mercury and antimony revealed orbital-scale dynamics of the Kuroshio Current. Quaternary Science Reviews 265, 107051. https://doi.org/10.1016/j.quascirev.2021.107051

Åkerblom, S., Bishop, K., Björn, E., Lambertsson, L., Eriksson, T., Nilsson, M.B., 2013. Significant interaction effects from sulfate deposition and climate on sulfur concentrations constitute major controls on methylmercury production in peatlands. Geochimica et Cosmochimica Acta 102, 1–11. https://doi.org/10.1016/j.gca.2012.10.025

Amos, H.M., Sonke, J.E., Obrist, D., Robins, N., Hagan, N., Horowitz, H.M., Mason, R.P., Witt, M., Hedgecock, I.M., Corbitt, E.S., Sunderland, E.M., 2015. Observational and modeling constraints on global anthropogenic enrichment of mercury. Environmental Science and Technology 49, 4036–4047. https://doi.org/10.1021/es5058665

Armenteros, I., 2010. Diagenesis of Carbonates in Continental Settings, in: Developments in Sedimentology. Elsevier, pp. 61–151. https://doi.org/10.1016/S0070-4571(09)06202-5

Armstrong, E., Tallavaara, M., Hopcroft, P.O., Valdes, P.J., 2023. North African humid periods over the past 800,000 years. Nat Commun 14, 5549. https://doi.org/10.1038/s41467-023-41219-4

Benoit, J.M., Gilmour, C.C., Mason, R.P., Heyes, A., 1999. Sulfide controls on mercury speciation and bioavailability to methylating bacteria in sediment pore waterA. Environmental Science and Technology 33, 1780. https://doi.org/10.1021/es992007q

Biester, H., Pérez-Rodríguez, M., Gilfedder, B.-S., Martínez Cortizas, A., Hermanns, Y.-M., 2018. Solar irradiance and primary productivity controlled mercury accumulation in sediments of a remote lake in the Southern Hemisphere during the past 4000 years: Primary productivity and mercury accumulation. Limnol. Oceanogr. 63, 540–549. https://doi.org/10.1002/lno.10647

Bin, C., Xiaoru, W., Lee, F.S.C., 2001. Pyrolysis coupled with atomic absorption spectrometry for the determination of mercury in Chinese medicinal materials. Analytica Chimica Acta 447, 161–169. https://doi.org/10.1016/S0003-2670(01)01218-1

Bishop, K., Shanley, J.B., Riscassi, A., de Wit, H.A., Eklöf, K., Meng, B., Mitchell, C., Osterwalder, S., Schuster, P.F., Webster, J., Zhu, W., 2020. Recent advances in understanding and measurement of mercury in the environment: Terrestrial Hg cycling. Science of the Total Environment 721. https://doi.org/10.1016/j.scitotenv.2020.137647

Blais, J.M., Kalff, J., 1995. The influence of lake morphometry on sediment focusing. Limnol. Oceanogr. 40, 582–588. https://doi.org/10.4319/lo.1995.40.3.0582

Boamah, D., Koeberl, C., 2007. The Lake Bosumtwi impact structure in Ghana: A brief environmental assessment and discussion of ecotourism potential. Meteoritics and Planetary Science 42, 561–567. https://doi.org/10.1111/j.1945-5100.2007.tb01061.x

Bradley, R.S., Diaz, H.F., 2021. Late Quaternary Abrupt Climate Change in the Tropics and Sub-Tropics: The Continental Signal of Tropical Hydroclimatic Events (THEs). Reviews of Geophysics 59, e2020RG000732. https://doi.org/10.1029/2020RG000732

Branfireun, B.A., Cosio, C., Poulain, A.J., Riise, G., Bravo, A.G., 2020. Mercury cycling in freshwater systems - An updated conceptual model. Science of the Total Environment 745. https://doi.org/10.1016/j.scitotenv.2020.140906

Bravo, A.G., Bouchet, S., Tolu, J., Björn, E., Mateos-Rivera, A., Bertilsson, S., 2017. Molecular composition of organic matter controls methylmercury formation in boreal lakes. Nat Commun 8, 14255. https://doi.org/10.1038/ncomms14255

Brodie, C.R., Leng, M.J., Casford, J.S.L., Kendrick, C.P., Lloyd, J.M., Yongqiang, Z., Bird, M.I., 2011. Evidence for bias in C and N concentrations and δ13C composition of terrestrial and aquatic organic materials due to pre-analysis acid preparation methods. Chemical Geology 282, 67–83. https://doi.org/10.1016/j.chemgeo.2011.01.007

Brooks, K., Scholz, C.A., King, J.W., Peck, J., Overpeck, J.T., Russell, J.M., Amoako, P.Y.O., 2005. Late-Quaternary lowstands of lake Bosumtwi, Ghana: Evidence from high-resolution seismic-reflection and sediment-core data. Palaeogeography, Palaeoclimatology, Palaeoecology 216, 235–249. https://doi.org/10.1016/j.palaeo.2004.10.005

Brumsack, H.J., 2006. The trace metal content of recent organic carbon-rich sediments: Implications for Cretaceous black shale formation. Palaeogeography, Palaeoclimatology, Palaeoecology 232, 344–361. https://doi.org/10.1016/j.palaeo.2005.05.011

Chang, M., Liu, B., Wang, B., Martinez-Villalobos, C., Ren, G., Zhou, T., 2022. Understanding Future Increases in Precipitation Extremes in Global Land Monsoon Regions. Journal of Climate 35, 1839–1851. https://doi.org/10.1175/JCLI-D-21-0409.1

Chede, B.S., Venancio, I.M., Figueiredo, T.S., Albuquerque, A.L.S., Silva-Filho, E.V., 2022. Mercury deposition in the western tropical South Atlantic during the last 70 ka. Palaeogeography, Palaeoclimatology, Palaeoecology 601, 111122. https://doi.org/10.1016/j.palaeo.2022.111122

Cohen, A., Campisano, C., Arrowsmith, R., Asrat, A., Behrensmeyer, A.K., Deino, A., Feibel, C., Hill, A., Johnson, R., Kingston, J., Lamb, H., Lowenstein, T., Noren, A., Olago, D., Owen, R.B., Potts, R., Reed,

K., Renaut, R., Schäbitz, F., Tiercelin, J.-J., Trauth, M.H., Wynn, J., Ivory, S., Brady, K., O'Grady, R., Rodysill, J., Githiri, J., Russell, J., Foerster, V., Dommain, R., Rucina, S., Deocampo, D., Russell, J., Billingsley, A., Beck, C., Dorenbeck, G., Dullo, L., Feary, D., Garello, D., Gromig, R., Johnson, T., Junginger, A., Karanja, M., Kimburi, E., Mbuthia, A., McCartney, T., McNulty, E., Muiruri, V., Nambiro, E., Negash, E.W., Njagi, D., Wilson, J.N., Rabideaux, N., Raub, T., Sier, M.J., Smith, P., Urban, J., Warren, M., Yadeta, M., Yost, C., Zinaye, B., 2016. The Hominin Sites and Paleolakes Drilling Project: inferring the environmental context of human evolution from eastern African rift lake deposits. Scientific Drilling 21, 1–16. https://doi.org/10.5194/sd-21-1-2016

Cohen, A.S., Campisano, C.J., Arrowsmith, J.R., Asrat, A., Beck, C.C., Behrensmeyer, A.K., Deino, A.L., Feibel, C.S., Foerster, V., Kingston, J.D., Lamb, H.F., Lowenstein, T.K., Lupien, R.L., Muiruri, V., Olago, D.O., Owen, R.B., Potts, R., Russell, J.M., Schaebitz, F., Stone, J.R., Trauth, M.H., Yost, C.L., 2022. Reconstructing the Environmental Context of Human Origins in Eastern Africa Through Scientific Drilling. Annu. Rev. Earth Planet. Sci. 50, 451–476. https://doi.org/10.1146/annurev-earth-031920-081947

Cohen, A.S., Stone, J.R., Beuning, K.R.M., Park, L.E., Reinthal, P.N., Dettman, D., Scholz, C.A., Johnson, T.C., King, J.W., Talbot, M.R., Brown, E.T., Ivory, S.J., 2007. Ecological consequences of early Late Pleistocene megadroughts in tropical Africa. PNAS U.S.A. 104, 16422–16427. https://doi.org/10.1073/pnas.0703873104

Cooke, C.A., Martínez-Cortizas, A., Bindler, R., Sexauer Gustin, M., 2020. Environmental archives of atmospheric Hg deposition – A review. Science of the Total Environment 709, 134800. https://doi.org/10.1016/j.scitotenv.2019.134800

Deplazes, G., Lückge, A., Peterson, L.C., Timmermann, A., Hamann, Y., Hughen, K.A., Röhl, U., Laj, C., Cane, M.A., Sigman, D.M., Haug, G.H., 2013. Links between tropical rainfall and North Atlantic climate during the last glacial period. Nature Geoscience 6, 213–217. https://doi.org/10.1038/ngeo1712

Edwards, B.A., Kushner, D.S., Outridge, P.M., Wang, F., 2021. Fifty years of volcanic mercury emission research: Knowledge gaps and future directions. Science of the Total Environment 757, 143800. https://doi.org/10.1016/j.scitotenv.2020.143800

Engstrom, D.R., Rose, N.L., 2013. A whole-basin, mass-balance approach to paleolimnology. J Paleolimnol 49, 333–347. https://doi.org/10.1007/s10933-012-9675-5

Fadina, O.A., Venancio, I.M., Belem, A., Silveira, C.S., Bertagnolli, D. de C., Silva-Filho, E.V., Albuquerque, A.L.S., 2019. Paleoclimatic controls on mercury deposition in northeast Brazil since the Last Interglacial. Quaternary Science Reviews 221, 105869. https://doi.org/10.1016/j.quascirev.2019.105869

Figueiredo, T.S., Bergquist, B.A., Santos, T.P., Albuquerque, A.L.S., Silva-Filho, E.V., 2022. Relationship between glacial CO2 drawdown and mercury cycling in the western South Atlantic: An isotopic insight. Geology 50, 3–7. https://doi.org/10.1130/g49942.1

Foerster, V., Asrat, A., Bronk Ramsey, C., Brown, E.T., Chapot, M.S., Deino, A., Duesing, W., Grove, M., Hahn, A., Junginger, A., Kaboth-Bahr, S., Lane, C.S., Opitz, S., Noren, A., Roberts, H.M., Stockhecke, M., Tiedemann, R., Vidal, C.M., Vogelsang, R., Cohen, A.S., Lamb, H.F., Schaebitz, F., Trauth, M.H., 2022. Pleistocene climate variability in eastern Africa influenced hominin evolution. Nature Geoscience 15, 805–811. https://doi.org/10.1038/s41561-022-01032-y

Francisco López, A., Heckenauer Barrón, E.G., Bello Bugallo, P.M., 2022. Contribution to understanding the influence of fires on the mercury cycle: Systematic review, dynamic modelling and application to sustainable hypothetical scenarios. Environmental Monitoring & Assessment 194, 707. https://doi.org/10.1007/s10661-022-10208-3

Frieling, J., Mather, T.A., März, C., Jenkyns, H.C., Hennekam, R., Reichart, G.-J., Slomp, C.P., Van Helmond, N.A.G.M., 2023. Effects of redox variability and early diagenesis on marine sedimentary Hg records. Geochimica et Cosmochimica Acta S0016703723001850. https://doi.org/10.1016/j.gca.2023.04.015

Gehrke, G.E., Blum, J.D., Meyers, P.A., 2009. The geochemical behavior and isotopic composition of Hg in a mid-Pleistocene western Mediterranean sapropel. Geochimica et Cosmochimica Acta 73, 1651–1665. https://doi.org/10.1016/j.gca.2008.12.012

Gosling, W.D., McMichael, C.N.H., Groenwoud, Z., Roding, E., Miller, C.S., Julier, A.C.M., 2021. Preliminary evidence for green, brown and black worlds in tropical western Africa during the Middle and Late Pleistocene. Palaeoecology of Africa 35, 13–25. https://doi.org/10.1201/9781003162766

Gosling, W.D., Miller, C.S., Shanahan, T.M., Holden, P.B., Overpeck, J.T., van Langevelde, Frank., 2022a. A stronger role for long-term moisture change than for CO2 in determining tropical woody vegetation change. Science 376, 653–656. https://doi.org/10.1126/science.abg4618

Gosling, W.D., Scerri, E.M.L., Kaboth-Bahr, S., 2022b. The climate and vegetation backdrop to hominin evolution in Africa. Philosophical Transactions of the Royal Society B: Biological Sciences 377. https://doi.org/10.1098/rstb.2020.0483

Grant, K.M., Amarathunga, U., Amies, J.D., Hu, P., Qian, Y., Penny, T., Rodriguez-Sanz, L., Zhao, X., Heslop, D., Liebrand, D., Hennekam, R., Westerhold, T., Gilmore, S., Lourens, L.J., Roberts, A.P., Rohling, E.J., 2022. Organic carbon burial in Mediterranean sapropels intensified during Green Sahara Periods since 3.2 Myr ago. Communications Earth & Environment 3, 11. https://doi.org/10.1038/s43247-021-00339-9

Grant, K.M., Grimm, R., Mikolajewicz, U., Marino, G., Ziegler, M., Rohling, E.J., 2016. The timing of Mediterranean sapropel deposition relative to insolation, sea-level and African monsoon changes. Quaternary Science Reviews 140, 125–141. https://doi.org/10.1016/j.quascirev.2016.03.026

1306 Grant, K.M., Rohling, E.J., Westerhold, T., Zabel, M., Heslop, D., Konijnendijk, T., Lourens, L., 2017. A 3 million
1307 year index for North African humidity/aridity and the implication of potential pan-African Humid periods.
1308 Quaternary Science Reviews 171, 100–118. https://doi.org/10.1016/j.quascirev.2017.07.005
1309 Grygar, T.M., Mach, K., Martinez, M., 2019. Checklist for the use of potassium concentrations in siliciclastic
1310 sediments as paleoenvironmental archives. Sedimentary Geology 382, 75–84.
1311 https://doi.org/10.1016/j.sedgeo.2019.01.010
1312 Guédron, S., Ledru, M.P., Escobar-Torrez, K., Develle, A.L., Brisset, E., 2018. Enhanced mercury deposition by
1313 Amazonian orographic precipitation: Evidence from high-elevation Holocene records of the Lake
1314 Titicaca region (Bolivia). Palaeogeography, Palaeoclimatology, Palaeoecology 511, 577–587.
1315 https://doi.org/10.1016/j.palaeo.2018.09.023
1316 Gulati, R.D., Zadereev, E.S., Degermendzhi, A.G. (Eds.), 2017. Ecology of Meromictic Lakes, Ecological Studies.
1317 Springer International Publishing, Cham. https://doi.org/10.1007/978-3-319-49143-1
1318 Gustin, M.S., Bank, M.S., Bishop, K., Bowman, K., Branfireun, B., Chételat, J., Eckley, C.S., Hammerschmidt,
1319 C.R., Lamborg, C., Lyman, S., Martínez-Cortizas, A., Sommar, J., Tsui, M.T.-K., Zhang, T., 2020.
1320 Mercury biogeochemical cycling: A synthesis of recent scientific advances. Science of The Total
1321 Environment 737, 139619. https://doi.org/10.1016/j.scitotenv.2020.139619
1322 Han, S., Obraztsova, A., Pretto, P., Deheyn, D.D., Gieskes, J., Tebo, B.M., 2008. Sulfide and iron control on
1323 mercury speciation in anoxic estuarine sediment slurries. Marine Chemistry 111, 214–220.
1324 https://doi.org/10.1016/j.marchem.2008.05.002
1325 Hermanns, Y.M., Biester, H., 2013. A 17,300-year record of mercury accumulation in a pristine lake in southern
1326 Chile. Journal of Paleolimnology 49, 547–561. https://doi.org/10.1007/s10933-012-9668-4
1327 Hermanns, Y.M., Cortizas, A.M., Arz, H., Stein, R., Biester, H., 2013. Untangling the influence of in-lake
1328 productivity and terrestrial organic matter flux on 4,250 years of mercury accumulation in Lake Hambre,
1329 Southern Chile. Journal of Paleolimnology 49, 563–573. https://doi.org/10.1007/s10933-012-9657-7
1330 Hernández, A., Martin-Puertas, C., Moffa-Sánchez, P., Moreno-Chamarro, E., Ortega, P., Blockley, S., Cobb, K.,
1331 Comas-Bru, L., Giralt, S., Goosse, H., Luterbacher, J., Martrat, B., Muscheler, R., Parnell, A., Pla-
1332 Rabes, S., Sjolte, J., Scaife, A., Swingedouw, D., Wise, E., Xu, G., 2020. Modes of climate variability:
1333 Synthesis and review of proxy-based reconstructions through the Holocene. Earth-Science Reviews
1334 209, 103286. https://doi.org/10.1016/j.earscirev.2020.103286
1335 Hsu-Kim, H., Kucharzyk, K.H., Zhang, T., Deshusses, M.A., 2013. Mechanisms Regulating Mercury
1336 Bioavailability for Methylating Microorganisms in the Aquatic Environment: A Critical Review.
1337 Environmental Science & Technology 47, 2441–2456. https://doi.org/10.1021/es304370g
1338 Jenkyns, H.C., 1988. The Early Toarcian (Jurassic) Anoxic Event. American Journal of Science.
1339 Jenkyns, H.C., Weedon, G.P., 2013. Chemostratigraphy ($CaCO_3$, TOC, $\delta^{13}C_{org}$) of Sinemurian (Lower Jurassic)
1340 black shales from the Wessex Basin, Dorset and palaeoenvironmental implications. Newsletters on
1341 Stratigraphy 46, 1–21. https://doi.org/10.1127/0078-0421/2013/0029
1342 Jeon, B., Scircle, A., Cizdziel, J.V., Chen, J., Black, O., Wallace, D.J., Zhou, Y., Lepak, R.F., Hurley, J.P., 2020.
1343 Historical deposition of trace metals in a marine sapropel from Mangrove Lake, Bermuda with emphasis
1344 on mercury, lead, and their isotopic composition. Journal of Soils & Sediments 20, 2266–2276.
1345 https://doi.org/10.1007/s11368-020-02567-6
1346 Jourdan, F., Renne, P.R., Reimold, W.U., 2009. An appraisal of the ages of terrestrial impact structures. Earth
1347 and Planetary Science Letters 286, 1–13. https://doi.org/10.1016/j.epsl.2009.07.009
1348 Kaboth-Bahr, S., Gosling, W.D., Vogelsang, R., Bahr, A., Scerri, E.M.L., 2021. Paleo-ENSO influence on African
1349 environments and early modern humans. PNAS 118, 1–6. https://doi.org/10.1073/pnas.2018277118
1350 Kiely, R., 2023. A 50,000-year reconstruction of West African fire history (MSc Thesis). University of Amsterdam,
1351 Amsterdam.
1352 Kinsley, C.W., Bradtmiller, L.I., McGee, D., Galgay, M., Stuut, J.B., Tjallingii, R., Winckler, G., DeMenocal, P.B.,
1353 2022. Orbital and Millennial-Scale Variability in Northwest African Dust Emissions Over the Past 67,000
1354 years. Paleoceanography and Paleoclimatology 37, 1–22. https://doi.org/10.1029/2020PA004137
1355 Koeberl, C., Milkereit, B., Overpeck, J.T., Scholz, C.A., Amoako, P.Y.O., Boamah, D., Danuor, S.K., Karp, T.,
1356 Kueck, J., Hecky, R.E., King, J.W., Peack, J.A., 2007. An international and multidisciplinary drilling
1357 project into a young complex impact structure: The 2004 ICDP Bosumtwi Crater Drilling Project - An
1358 overview. Meteoritics and Planetary Science 42, 483–511. https://doi.org/10.1111/j.1945-
1359 5100.2007.tb01057.x
1360 Koeberl, C., Peck, J., King, J., Milkereit, B., Overpeck, J., Scholz, C., 2005. The ICDP lake Bosumtwi drilling
1361 project: A first report. Scientific Drilling 1, 23–27. https://doi.org/10.2204/iodp.sd.1.04.2005
1362 Kuss, J., Zülicke, C., Pohl, C., Schneider, B., 2011. Atlantic mercury emission determined from continuous
1363 analysis of the elemental mercury sea-air concentration difference within transects between 50°N and
1364 50°S. Global Biogeochemical Cycles 25. https://doi.org/10.1029/2010GB003998
1365 Larrasoaña, J.C., Roberts, A.P., Rohling, E.J., 2013. Dynamics of Green Sahara Periods and Their Role in
1366 Hominin Evolution. PLoS ONE 8. https://doi.org/10.1371/journal.pone.0076514
1367 Laskar, J., Robutel, P., Joutel, F., Gastineau, M., Correia, A.C.M., Levrard, B., 2004. A long-term numerical
1368 solution for the insolation quantities of the Earth. Astronomy and Astrophysics 428, 261–285.
1369 https://doi.org/10.1051/0004-6361:20041335
1370 Leiva González, J., Diaz-Robles, L.A., Cereceda-Balic, F., Pino-Cortés, E., Campos, V., 2022. Atmospheric
1371 Modelling of Mercury in the Southern Hemisphere and Future Research Needs: A Review. Atmosphere
1372 13, 1226. https://doi.org/10.3390/atmos13081226

Formatted: German (Switzerland)

Formatted: French (Switzerland)

Lent, R.M., Alexander, C.R., 1996. Mercury accumulation in Devils Lake, north Dakota - effects of environmental variation in closed-basin lakes on mercury chronologies. Water, Air, & Soil Pollution 98, 275–296.

Lézine, A.-M., Izumi, K., Kageyama, M., Achoundong, G., 2019. A 90,000-year record of Afromontane forest responses to climate change. Science 363, 177–181. https://doi.org/10.1126/science.aav6821

Li, F., Ma, C., Zhang, P., 2020. Mercury Deposition, Climate Change and Anthropogenic Activities: A Review. Frontiers in Earth Science 8, 316. https://doi.org/10.3389/feart.2020.00316

Lisiecki, L.E., Raymo, M.E., 2005. A Pliocene-Pleistocene stack of 57 globally distributed benthic δ 18O records. Paleoceanography 20, 1–17. https://doi.org/10.1029/2004PA001071

Liu, M., Zhang, Q., Maavara, T., Liu, S., Wang, X., Raymond, P.A., 2021. Rivers as the largest source of mercury to coastal oceans worldwide. Nature Geoscience 14, 672–677. https://doi.org/10.1038/s41561-021-00793-2

Lyman, S.N., Cheng, I., Gratz, L.E., Weiss-Penzias, P., Zhang, L., 2020. An updated review of atmospheric mercury. Science of the Total Environment 707, 135575. https://doi.org/10.1016/j.scitotenv.2019.135575

Machado, W., Sanders, C.J., Santos, I.R., Sanders, L.M., Silva-Filho, E.V., Luiz-Silva, W., 2016. Mercury dilution by autochthonous organic matter in a fertilized mangrove wetland. Environmental Pollution 213, 30–35. https://doi.org/10.1016/j.envpol.2016.02.002

Mason, R.P., Laporte, J.M., Andres, S., 2000. Factors controlling the bioaccumulation of mercury, methylmercury, arsenic, selenium, and cadmium by freshwater invertebrates and fish. Archives of Environmental Contamination and Toxicology 38, 283–297. https://doi.org/10.1007/s002449910038

McKay, N.P., 2012. A multidisciplinary approach to late Quaternary paleoclimatology with an emphasis on sub-saharan West Africa and the last interglacial period (PhD Thesis). University of Arizona, Arizona.

Menviel, L., Govin, A., Avenas, A., Meissner, K.J., Grant, K.M., Tzedakis, P.C., 2021. Drivers of the evolution and amplitude of African Humid Periods. Communications Earth & Environment 2, 237. https://doi.org/10.1038/s43247-021-00309-1

Miller, C.S., Gosling, W.D., 2014. Quaternary forest associations in lowland tropical West Africa. Quaternary Science Reviews 84, 7–25. https://doi.org/10.1016/j.quascirev.2013.10.027

Miller, C.S., Gosling, W.D., Kemp, D.B., Coe, A.L., Gilmour, I., 2016. Drivers of ecosystem and climate change in tropical West Africa over the past ~540 000 years. Journal of Quaternary Science 31, 671–677. https://doi.org/10.1002/jqs.2893

Moore, H.R., Crocker, A.J., Belcher, C.M., Meckler, A.N., Osborne, C.P., Beerling, D.J., Wilson, P.A., 2022. Hydroclimate variability was the main control on fire activity in northern Africa over the last 50,000 years. Quaternary Science Reviews 288, 107578. https://doi.org/10.1016/j.quascirev.2022.107578

Nalbant, J., Schneider, L., Hamilton, R., Connor, S., Biester, H., Stuart-Williams, H., Bergal-Kuvikas, O., Jacobsen, G., Stevenson, J., 2023. Fire, volcanism and climate change: the main factors controlling mercury (Hg) accumulation rates in Tropical Lake Lantoa, Sulawesi, Indonesia (~16,500–540 cal yr BP). Frontiers in Environmental Chemistry 4, 1241176. https://doi.org/10.3389/fenvc.2023.1241176

Nicholson, S.E., 2013. The West African Sahel: A Review of Recent Studies on the Rainfall Regime and Its Interannual Variability. ISRN Meteorology 2013, 1–32. https://doi.org/10.1155/2013/453521

Obrist, D., Kirk, J.L., Zhang, L., Sunderland, E.M., Jiskra, M., Selin, N.E., 2018. A review of global environmental mercury processes in response to human and natural perturbations: Changes of emissions, climate, and land use. Ambio 47, 116–140. https://doi.org/10.1007/s13280-017-1004-9

Outridge, P.M., Stern, G.A., Hamilton, P.B., Sanei, H., 2019. Algal scavenging of mercury in preindustrial Arctic lakes. Limnology & Oceanography 64, 1558–1571. https://doi.org/10.1002/lno.11135

Outridge, Sanei, H., Stern, Hamilton, Goodarzi, F., 2007. Evidence for Control of Mercury Accumulation Rates in Canadian High Arctic Lake Sediments by Variations of Aquatic Primary Productivity. Environmental Science & Technology 41, 5259–5265. https://doi.org/10.1021/es070408x

Paine, A.R., Fendley, I.M., Frieling, J., Mather, T.A., Lacey, J.H., Wagner, B., Robinson, S.A., Pyle, D.M., Francke, A., Them II, T.R., Panagiotopoulos, K., 2024. Mercury records covering the past 90 000 years from lakes Prespa and Ohrid, SE Europe. Biogeosciences 21, 531–556. https://doi.org/10.5194/bg-21-531-2024

Pan, J., Zhong, W., Wei, Z., Ouyang, J., Shang, S., Ye, S., Chen, Y., Xue, J., Tang, X., 2020. A 15,400-year record of natural and anthropogenic input of mercury (Hg) in a sub-alpine lacustrine sediment succession from the western Nanling Mountains, South China. Environmental Science and Pollution Research 27, 20478–20489. https://doi.org/10.1007/s11356-020-08421-z

Pausata, F.S.R., Gaetani, M., Messori, G., Berg, A., Maia de Souza, D., Sage, R.F., deMenocal, P.B., 2020. The Greening of the Sahara: Past Changes and Future Implications. One Earth 2, 235–250. https://doi.org/10.1016/j.oneear.2020.03.002

Peck, J.A., Green, R.R., Shanahan, T., King, J.W., Overpeck, J.T., Scholz, C.A., 2004. A magnetic mineral record of Late Quaternary tropical climate variability from Lake Bosumtwi, Ghana. Palaeogeography, Palaeoclimatology, Palaeoecology 215, 37–57. https://doi.org/10.1016/j.palaeo.2004.08.003

Pérez-Rodríguez, M., Margalef, O., Corella, J.P., Saiz-Lopez, A., Pla-Rabes, S., Giralt, S., Cortizas, A.M., 2018. The role of climate: 71 ka of atmospheric mercury deposition in the southern hemisphere recorded by Rano Aroi Mire, Easter Island (Chile). Geosciences (Switzerland) 8. https://doi.org/10.3390/geosciences8100374

Pilla, R.M., Williamson, C.E., Adamovich, B.V., Adrian, R., Anneville, O., Chandra, S., Colom-Montero, W., Devlin, S.P., Dix, M.A., Dokulil, M.T., Gaiser, E.E., Girdner, S.F., Hambright, K.D., Hamilton, D.P., Havens, K., Hessen, D.O., Higgins, S.N., Huttula, T.H., Huuskonen, H., Isles, P.D.F., Joehnk, K.D.,

Jones, I.D., Keller, W.B., Knoll, L.B., Korhonen, J., Kraemer, B.M., Leavitt, P.R., Lepori, F., Luger, M.S., Maberly, S.C., Melack, J.M., Melles, S.J., Müller-Navarra, D.C., Pierson, D.C., Pislegina, H.V., Plisnier, P.-D., Richardson, D.C., Rimmer, A., Rogora, M., Rusak, J.A., Sadro, S., Salmaso, N., Saros, J.E., Saulnier-Talbot, É., Schindler, D.E., Schmid, M., Shimaraeva, S.V., Silow, E.A., Sitoki, L.M., Sommaruga, R., Straile, D., Strock, K.E., Thiery, W., Timofeyev, M.A., Verburg, P., Vinebrooke, R.D., Weyhenmeyer, G.A., Zadereev, E., 2020. Deeper waters are changing less consistently than surface waters in a global analysis of 102 lakes. Scientific Reports 10, 20514. https://doi.org/10.1038/s41598-020-76873-x

Pompeani, D.P., Cooke, C.A., Abbott, M.B., Drevnick, P.E., 2018. Climate, Fire, and Vegetation Mediate Mercury Delivery to Midlatitude Lakes over the Holocene. Environmental Science and Technology 52, 8157–8164. https://doi.org/10.1021/acs.est.8b01523

Ravichandran, M., 2004. Interactions between mercury and dissolved organic matter - A review. Chemosphere 55, 319–331. https://doi.org/10.1016/j.chemosphere.2003.11.011

Russell, J., Talbot, M.R., Haskell, B.J., 2003. Mid-holocene climate change in Lake Bosumtwi, Ghana. Quaternary Research 60, 133–141. https://doi.org/10.1016/S0033-5894(03)00065-6

Sanei, H., Grasby, S., Beauchamp, B., 2012. Latest Permian mercury anomalies. Geology 40, 63–66.

Schneider, L., Cooke, C.A., Stansell, N.D., Haberle, S.G., 2020. Effects of climate variability on mercury deposition during the Older Dryas and Younger Dryas in the Venezuelan Andes. Journal of Paleolimnology 63, 211–224. https://doi.org/10.1007/s10933-020-00111-7

Schneider, L., Fisher, J.A., Diéguez, M.C., Fostier, A.-H., Guimaraes, J.R.D., Leaner, J.J., Mason, R., 2023. A synthesis of mercury research in the Southern Hemisphere, part 1: Natural processes. Ambio 52, 897–917. https://doi.org/10.1007/s13280-023-01832-5

Scholz, C.A., Johnson, T.C., Cohen, A.S., King, J.W., Peck, J.A., Overpeck, J.T., Talbot, M.R., Brown, E.T., Kalindekafe, L., Amoako, P.Y.O., Lyons, R.P., Shanahan, T.M., Castañeda, I.S., Heil, C.W., Forman, S.L., McHargue, L.R., Beuning, K.R., Gomez, J., Pierson, J., 2007. East African megadroughts between 135 and 75 thousand years ago and bearing on early modern human origins. PNAS USA 104, 16416–16421. https://doi.org/10.1073/pnas.0703874104

Schultze, M., Boehrer, B., Wendt-Potthoff, K., Katsev, S., Brown, E.T., 2017. Chemical Setting and Biogeochemical Reactions in Meromictic Lakes, in: Ecology of Meromictic Lakes. Springer, pp. 35–61.

Schütze, M., Gatz, P., Gilfedder, B., Biester, H., 2021. Why productive lakes are larger mercury sedimentary sinks than oligotrophic brown water lakes. Limnology & Oceanography 66, 1316–1332. https://doi.org/10.1002/lno.11684

Schütze, M., Tserendorj, G., Pérez-Rodríguez, M., Rösch, M., Biester, H., 2018. Prediction of Holocene mercury accumulation trends by combining palynological and geochemical records of lake sediments (Black Forest, Germany). Geosciences (Switzerland) 8. https://doi.org/10.3390/geosciences8100358

Sebag, D., Garcin, Y., Adatte, T., Deschamps, P., Ménot, G., Verrecchia, E.P., 2018. Correction for the siderite effect on Rock-Eval parameters: Application to the sediments of Lake Barombi (southwest Cameroon). Organic Geochemistry 123, 126–135. https://doi.org/10.1016/j.orggeochem.2018.05.010

Segato, D., Saiz-Lopez, A., Mahajan, A.S., Wang, F., Corella, J.P., Cuevas, C.A., Erhardt, T., Jensen, C.M., Zeppenfeld, C., Kjær, H.A., Turetta, C., Cairns, W.R.L., Barbante, C., Spolaor, A., 2023. Arctic mercury flux increased through the Last Glacial Termination with a warming climate. Nature Geoscience 16, 439–445. https://doi.org/10.1038/s41561-023-01172-9

Selin, N.E., 2009. Global biogeochemical cycling of mercury: a review. Annual Review of Environmental Resources 34, 43–63.

Shanahan, T.M., Beck, J.W., Overpeck, J.T., McKay, N.P., Pigati, J.S., Peck, J.A., Scholz, C.A., Heil, C.W., King, J., 2012. Late Quaternary sedimentological and climate changes at Lake Bosumtwi Ghana: New constraints from laminae analysis and radiocarbon age modeling. Palaeogeography, Palaeoclimatology, Palaeoecology 361–362, 49–60. https://doi.org/10.1016/j.palaeo.2012.08.001

Shanahan, T.M., Mckay, N.P., Hughen, K.A., Overpeck, J.T., Otto-Bliesner, B., Heil, C.W., King, J., Scholz, C.A., Peck, J., 2015. The time-transgressive termination of the African humid period. Nature Geoscience 8, 140–144. https://doi.org/10.1038/ngeo2329

Shanahan, T.M., Overpeck, J.T., Anchukaitis, K.J., Beck, J.W., Cole, J.E., Dettman, D.L., Peck, J.A., Scholz, C.A., King, J.W., 2009. Atlantic forcing of persistent drought in West Africa. Science 324, 377–380. https://doi.org/10.1126/science.1166352

Shanahan, T.M., Overpeck, J.T., Beck, J.W., Wheeler, C.W., Peck, J.A., King, J.W., Scholz, C.A., 2008a. The formation of biogeochemical laminations in Lake Bosumtwi, Ghana, and their usefulness as indicators of past environmental changes. Journal of Paleolimnology 40, 339–355. https://doi.org/10.1007/s10933-007-9164-4

Shanahan, T.M., Overpeck, J.T., Scholz, C.A., Beck, J.W., Peck, J., King, J.W., 2008b. Abrupt changes in the water balance of tropical West Africa during the late Quaternary. Journal of Geophysical Research 113, D12108. https://doi.org/10.1029/2007JD009320

Shanahan, T.M., Overpeck, J.T., Sharp, W.E., Scholz, C.A., Arko, J.A., 2007. Simulating the response of a closed-basin lake to recent climate changes in tropical West Africa (Lake Bosumtwi, Ghana). Hydrological Processes 21, 1678–1691. https://doi.org/10.1002/hyp.6359

Shanahan, T.M., Overpeck, J.T., Wheeler, C.W., Beck, J.W., Pigati, J.S., Talbot, M.R., Scholz, C.A., Peck, J., King, J.W., 2006. Paleoclimatic variations in West Africa from a record of late Pleistocene and Holocene

1506   lake level stands of Lake Bosumtwi, Ghana. Palaeogeography, Palaeoclimatology, Palaeoecology 242,
1507   287–302. https://doi.org/10.1016/j.palaeo.2006.06.007
1508 Shanahan, T.M., Peck, J.A., McKay, N., Heil, C.W., King, J., Forman, S.L., Hoffmann, D.L., Richards, D.A.,
1509   Overpeck, J.T., Scholz, C., 2013. Age models for long lacustrine sediment records using multiple dating
1510   approaches - An example from Lake Bosumtwi, Ghana. Quaternary Geochronology 15, 47–60.
1511   https://doi.org/10.1016/j.quageo.2012.12.001
1512 Shen, J., Feng, Q., Algeo, T.J., Liu, Jinling, Zhou, C., Wei, W., Liu, Jiangsi, Them, T.R., Gill, B.C., Chen, J., 2020.
1513   Sedimentary host phases of mercury (Hg) and implications for use of Hg as a volcanic proxy. Earth and
1514   Planetary Science Letters 543, 116333. https://doi.org/10.1016/j.epsl.2020.116333
1515 Skonieczny, C., McGee, D., Winckler, G., Bory, A., Bradtmiller, L.I., Kinsley, C.W., Polissar, P.J., De Pol-Holz, R.,
1516   Rossignol, L., Malaizé, B., 2019. Monsoon-driven Saharan dust variability over the past 240,000 years.
1517   Science Advances 5, 1–9. https://doi.org/10.1126/sciadv.aav1887
1518 Soerensen, A.L., Mason, R.P., Balcom, P.H., Jacob, D.J., Zhang, Y., Kuss, J., Sunderland, E.M., 2014.
1519   Elemental Mercury Concentrations and Fluxes in the Tropical Atmosphere and Ocean. Environmental
1520   Science & Technology 48, 11312–11319. https://doi.org/10.1021/es503109p
1521 Sprovieri, F., Pirrone, N., Bencardino, M., D'Amore, F., Angot, H., Barbante, C., Brunke, E.-G., Arcega-Cabrera,
1522   F., Cairns, W., Comero, S., Diéguez, M. del C., Dommergue, A., Ebinghaus, R., Feng, X.B., Fu, X.,
1523   Garcia, P.E., Gawlik, B.M., Hageström, U., Hansson, K., Horvat, M., Kotnik, J., Labuschagne, C.,
1524   Magand, O., Martin, L., Mashyanov, N., Mkololo, T., Munthe, J., Obolkin, V., Ramirez Islas, M., Sena,
1525   F., Somerset, V., Spandow, P., Vardè, M., Walters, C., Wängberg, I., Weigelt, A., Yang, X., Zhang, H.,
1526   2017. Five-year records of mercury wet deposition flux at GMOS sites in the Northern and Southern
1527   hemispheres. Atmospheric Chemistry & Physics 17, 2689–2708. https://doi.org/10.5194/acp-17-2689-
1528   2017
1529 Sprovieri, F., Pirrone, N., Ebinghaus, R., Kock, H., Dommergue, A., 2010. A review of worldwide atmospheric
1530   mercury measurements. Atmospheric Chemistry and Physics 10, 8245–8265.
1531   https://doi.org/10.5194/acp-10-8245-2010
1532 Swart, P.K., 2015. The geochemistry of carbonate diagenesis: The past, present and future. Sedimentology 62,
1533   1233–1304. https://doi.org/10.1111/sed.12205
1534 Talbot, M.R., Johannessen, T., 1992. A high resolution palaeoclimatic record for the last 27,500 years in tropical
1535   West Africa from the carbon and nitrogen isotopic composition of lacustrine organic matter. Earth and
1536   Planetary Science Letters 110, 23–37. https://doi.org/10.1016/0012-821X(92)90036-U
1537 Them, T.R., Jagoe, C.H., Caruthers, A.H., Gill, B.C., Grasby, S.E., Gröcke, D.R., Yin, R., Owens, J.D., 2019.
1538   Terrestrial sources as the primary delivery mechanism of mercury to the oceans across the Toarcian
1539   Oceanic Anoxic Event (Early Jurassic). Earth and Planetary Science Letters 507, 62–72.
1540   https://doi.org/10.1016/j.epsl.2018.11.029
1541 Tisserand, D., Guédron, S., Viollier, E., Jézéquel, D., Rigaud, S., Campillo, S., Sarret, G., Charlet, L., Cossa, D.,
1542   2022. Mercury, organic matter, iron, and sulfur co-cycling in a ferruginous meromictic lake. Applied
1543   Geochemistry 146, 105463. https://doi.org/10.1016/j.apgeochem.2022.105463
1544 Tjallingii, R., Claussen, M., Stuut, J.-B.W., Fohlmeister, J., Jahn, A., Bickert, T., Lamy, F., Röhl, U., 2008.
1545   Coherent high- and low-latitude control of the northwest African hydrological balance. Nature
1546   Geoscience 1, 670–675. https://doi.org/10.1038/ngeo289
1547 Trauth, M.H., Asrat, A., Berner, N., Bibi, F., Foerster, V., Grove, M., Kaboth-Bahr, S., Maslin, M.A., Mudelsee, M.,
1548   Schäbitz, F., 2021. Northern Hemisphere Glaciation, African climate and human evolution. Quaternary
1549   Science Reviews 268, 107095. https://doi.org/10.1016/j.quascirev.2021.107095
1550 Tribovillard, N., Algeo, T.J., Lyons, T., Riboulleau, A., 2006. Trace metals as paleoredox and paleoproductivity
1551   proxies: An update. Chemical Geology 232, 12–32. https://doi.org/10.1016/j.chemgeo.2006.02.012
1552 Turner, B.F., Gardner, L.R., Sharp, W.E., 1996. The hydrology of lake Bosumtwi, a climate-sensitive lake in
1553   Ghana, West Africa. Journal of Hydrology 183, 243–261. https://doi.org/10.1016/0022-1694(95)02982-6
1554 United Nations Environment Programme, 2018. Global Mercury Assessment, United Nations.
1555 Vindušková, O., Jandová, K., Frouz, J., 2019. Improved method for removing siderite by *in situ* acidification
1556   before elemental and isotope analysis of soil organic carbon. Journal of Plant Nutrition and Soil Science
1557   182, 82–91. https://doi.org/10.1002/jpln.201800164
1558 Weldeab, S., Lea, D.W., Schneider, R.R., Andersen, N., 2007. 155,000 Years of West African Monsoon and
1559   Ocean Thermal Evolution. Science 316, 1303–1307. https://doi.org/10.1126/science.1140461
1560 White, F. (Frank), 1983. The vegetation of Africa: a descriptive memoir to accompany the
1561   Unesco/AETFAT/UNSO vegetation map of Africa, Natural resources research ; 20. Unesco, Paris.
1562 Woolway, R.I., Kraemer, B.M., Lenters, J.D., Merchant, C.J., O'Reilly, C.M., Sharma, S., 2020. Global lake
1563   responses to climate change. Nature Reviews Earth and Environment 1, 388–403.
1564   https://doi.org/10.1038/s43017-020-0067-5
1565 Zaferani, S., Biester, H., 2021. Mercury Accumulation in Marine Sediments – A Comparison of an Upwelling Area
1566   and Two Large River Mouths. Frontiers in Marine Science 8, 732720.
1567   https://doi.org/10.3389/fmars.2021.732720
1568 Zolitschka, B., Francus, P., Ojala, A.E.K., Schimmelmann, A., 2015. Varves in lake sediments – a review.
1569   Quaternary Science Reviews 117, 1–41.
1570 Zou, J., Chang, Y.P., Zhu, A., Chen, M.T., Kandasamy, S., Yang, H., Cui, J., Yu, P.S., Shi, X., 2021. Sedimentary
1571   mercury and antimony revealed orbital-scale dynamics of the Kuroshio Current. Quaternary Science
1572   Reviews 265, 107051. https://doi.org/10.1016/j.quascirev.2021.107051

1573